MIDLATITUDE MESOSCALE CONVECTIVE COMPLEX PRECIPITATION CYCLES AND STRUCTURES

by

ROBERT PATRICK CALLAHAN

B.S., Texas A&M University

(1979)

Submitted to the Department of

Meteorology and Physical Oceanography

in Partial Fulfillment of the

Requirements of the

Degree of

MASTER OF SCIENCE

at the

MASSACHUSETTS INSTITUTE OF TECHNOLOGY

May 1983

Signature of Author: _____

Department of Meteorology and Physical Oceanography, 18 May 1983

Certified by: _____

Frederick Sanders, Thesis Supervisor

Accepted by: _____

Ronald George Prinn, Chairman, Meteorology and Physical Oceanography Departmental Committee

MIDLATITUDE MESOSCALE CONVECTIVE COMPLEX

PRECIPITATION CYCLES AND STRUCTURE

by

ROBERT PATRICK CALLAHAN

Submitted to the Department of

Meteorology and Physical Oceanography

in Partial Fulfillment of the

Requirements of the

Degree of

Master of Science

ABSTRACT

The precipitation cycles and structures of sixteen Mesoscale Convective Complexes (MCCs) from the warm seasons of 1978 and 1979, and August 1982 were studied. Manually digitized radar data from the National Weather Service 10 cm radar network was primarily used. A large subclass of the MCCs examined were found to have consistently observable precipitation cycles and structures. In the early phase, the precipitation of an MCC is nearly identical to the structure of a tropical squall line, while in the late phase, the active regions have characteristics of a weak midlatitude squall line. Meso-circulations, particularly a mesolow which forms in the lower troposphere, appear responsible for this change in precipitation structure. The usefulness of classifying MCCs as unique organized mesoscale convection was discussed.

Thesis Supervisor: Dr. Frederick Sanders, Professor of Meteorology

CONTENTS

FIGURES AND TABLES

Figures

Tables

1. Introduction

By documenting convective and stratiform precipitation cycles and structures then integrating this knowledge into the structures and models elucidated by other researchers, a better understanding of the Mesoscale Convective Complex (MCC) is obtained. National Weather Service network radar data was used for the bulk of this study. This operational data was chosen because no research radar data covering the entire lifetime of the MCC is known to exist. Although the author could not control the quality of each radar observation, the data was taken using mostly standardized procedures, then put into numerical form. Standardized procedures and numerical data are conducive to scientific research.

2. Radar data

Radar observation logs for each station of the National Weather Service network of WSR-57 10 cm radars were obtained. Observations on the logs were taken hourly, 35 minutes past each hour, by the observer at each station, in a digital form. The digital information was obtained by laying a grid over the plan position indicator (PPI) and noting the maximum observed intensity in each box containing echoes of moderate or greater intensity. If light intensity was the greatest intensity observed in a grid box, it was reported only if more that 20% of the box was covered. Intensities were reported with code numbers 1 to 6 and correspond to the dBZ levels in Table 1. Two other numbers, 8 and 9, were sometimes reported; they signify echoes of unknown intensities observed beyond the maximum intensity measuring range, 232 km, of the radar. In this study, 8 and 9 were always assigned the value 1 because they occurred on the periphery of the MCC precipitation. Overlapping radar coverage was sufficient to rule out the possibility of higher intensities going unobserved in most cases.

Hourly digital data from all stations was plotted on a subgrid of the Limited Fine Mesh (LFM) grid. Each subgrid has one-fourth the mesh length of the LFM, a side of approximately 40 km, and an area of about 1600 km^2. Whenever data from more than one station was entered at the same box, the data of highest value was plotted. Determining which data belonged to an MCC was generally easy because the data would be closely spaced and under the cloud shield observed in infrared (IR) satellite pictures. In the cases where closeby data was not considered MCC related, analysis including these generally small amounts of data did not make significant changes in

Table 1. Definition of intensity levels. Intervals of dBZ from U.S. Dept. of Commerce (1978). Rainfall rates derived from Z-R relationship $Z=200R^{1.6}$ as modified in text

Intensity Level	Echo Intensity	dBZ	Rainfall Rate (mm/h)
6	Extreme	$\geq$57	75
5	Intense	50-56	50
4	Very Strong	45-49	25
3	Strong	41-44	13
2	Moderate	30-40	3
1	Weak	$\leq$29	1

the results.

Once the MCC data was isolated, each datum was designated as either stratiform or convective rain. By observing that most of the uniform, stratiform-like areas were either 1's or 2's, the clumpy, convection-like areas, 3 and above, and with the knowledge that the highest intensities are convective, a simple procedure was devised where boxes containing 1 or 2 were considered stratiform rain and 3 to 6 convective rain. A similar approach was used by Houze (1977) in his study of a tropical squall line system.

The weakness in using this digitized radar data is twofold. First, the grid size is so large, it will tend to overestimate the area of rain. This is especially true in the case of convection where a single convective cell of, say 50 km^2 could cause a grid box of 1600 km^2 to be considered convective. Second, the intensity value reported for each grid box is the maximum observed intensity, and it is not known exactly what the relationship is between the maximum value and the mean, especially with respect to convection, except that this maximum observed intensity is overestimating the mean intensity for the grid box.

Problems of overestimation were overcome in the following ways: the often used Z-R relationship,

$$Z=200R^{1.6}, \qquad (1)$$

where radar reflectivity factor $Z(mm^6/m^3)$ and rainfall rate R(mm/h), was used, which gives realistic values for stratiform rain, but slightly underestimates convective rain and takes into account that each grid value is used as an estimate over an hour. The original intensity observation could have fallen anywhere within the range of dBZ for a particular intensity level, but, again, to make a closer estimate to the mean

intensity, the rainfall rate for the lowest value of dBZ in an intensity level was used. Additionally, the rainfall rate for level 1 was given a nominal value of 1 mm/h, and level 6 was limited to 75 mm/h because of the likely presence of hail, which can add to the reflectivity without adding much to the rainfall rate.

To check these correction factors, the hourly total rain rates (kg/h) for the MCC of 19/20 June 1978 were painstakingly computed from Environmental Data and Information Service Hourly Precipitation Data and compared with the radar-derived rates. Hourly radar-derived stratiform rainfall rates can be considered a reasonable estimate for many reasons, including : (1) the ratio of the area of a grid box to the area of the rain in an MCC is approximately 1/100, (2) in widespread rain the difference between the maximum observed value of reflectivity in a grid box and the mean is small, and (3) on the edge of the rain the observing rules eliminate light rain areas of less that 20% coverage. Because these radar-derived stratiform rain rates are a good estimate, overestimates of total rain rates come from inaccuracies in the convective estimate, and a final correction factor of .36 was computed. This correction factor, when multiplied times the convective rain rates, causes the sum of the stratiform and convective rain rates to equal the total rain rates observed on the ground. Due to missing data in the early part of the June 1978 MCC, the final correction factor was derived only from the last eight hours of precipitation data. Since the correction factor was derived from only a part of a single storm, and not the May 1979 storm presented in this paper, plots of convective and stratiform rain rates should be viewed carefully when their relative magnitudes are compared.

3. Selection of MCCs for study

The MCCs for the warm seasons of 1978 and 1979 identified by Maddox (1980,1981) and MCCs which occurred in August and September 1982 form the basis of this study. This group was reduced to sixteen cases because of data availability, and an attempt to sample storms of various size, duration and months throughout the warm season (Table 2). It includes four of the ten MCCs Maddox (1981) used in making his composite storm. Although the sixteen cases were examined to varying degrees, only the cases of 19/20 May 1979 and 26/27 August 1982 will be included in this paper, These two cases do not represent all the possible MCC precipitation configurations, but both cases are similar to those MCCs used to create Maddox' composite storm. The May 1979(B) case best exhibits the most fundamental characteristics of the sixteen storms, and the 26/27 August 1982 case clearly demonstrates an important phase in the life of the MCC.

Table 2. List of MCCs and Types of Data Available in the study

	DATA		
Date	Satellite	Facsimile Maps	Digital Radar
6/7 MAY 78	X	X	X
19/20 MAY 79(A)	X	X	X
19/20 MAY 79(B)	X	X	X
2/3 JUN 78	X	X	
3/4 JUN 78	X	X	
19/20 JUN 78	X	X	X
21/22 JUN 79	X	X	
22/23 JUN 79(A)	X	X	
22/23 JUN 79(B)	X	X	
1/2 JUL 78	X	X	X
6 JUL 78	X	X	X
13 JUL 78	X	X	X
19/20 JUL 78	X	X	X
24/25 AUG 82	X	X	
26/27 AUG 82	X	X	X
31 AUG/1 SEP 82	X	X	

4. Radar time series

Figs. 1-7 display the results of the analysis of the hourly radar maps for the MCC of 19/20 May 1979(B). In Fig. 1, the total area (convective plus stratiform) covered by rain is plotted against time. The times when the storm met Maddox' (1980) criteria are plotted at the top of the graph. Note the roughly four stages in the plotted data: 1800-0000 GMT, little growth, 0000-1000 GMT, strong growth; and, after 1000GMT, slow decay. Other storms exhibited similar behavior, with the differences occurring in the slopes of the strong growth and decay, and in the height of the peaks.

Fig. 2 shows total area-integrated rainfall rate or rain rate (kg/h) over the area and life of the MCC. The distinguishing features are the rapid growth, peak (occurring somewhat before maximum cloud extent), and decay. Examination of other storms reveals slight differences in the placement of the peak before maximum cloud extent and slightly different slopes for growth and decay.

The final graph in this subgroup, Fig. 3, is a plot of the area-averaged rainfall rate or intensity, and is computed by averaging all of the observed intensities. Most MCCs do not have this overall symmetrical form; there is usually a rapid build up to a peak then a slower decay.

A trend is evident in this data which will become more apparent in the next set of graphs, i.e., a peak in the intensity, followed by a peak in the rain rate, and finally a peak in the area affected.

Processes affecting the storm's life become more evident once the data is divided into convective and stratiform parts. Fig. 4 shows the area covered by convective rain along with a plot of stratiform rain area. The first significant period occurs between 0100-0800 GMT which shows a steady

Figure 1. Total area of rain, MCC of 19/20 May 1979(B). I, ME, and T mark Maddox' times of initiation, maximum extent, and termination, respectively.

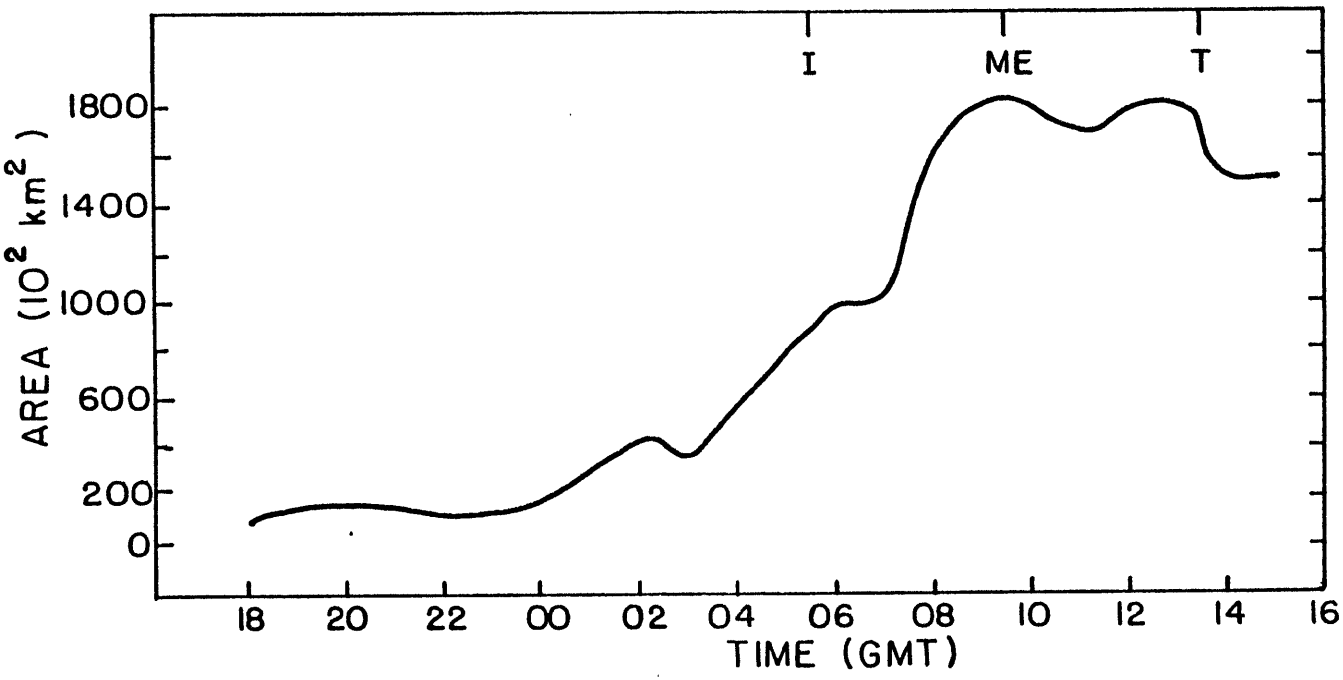
I
ME
T
1800
1400
1000
600
200
0
AREA (10^2 km^2)
18
20
22
00
02
04
06
08
10
12
14
16
TIME (GMT)

Figure 2. Total rain rate, MCC of 19/20 May 1979(B).

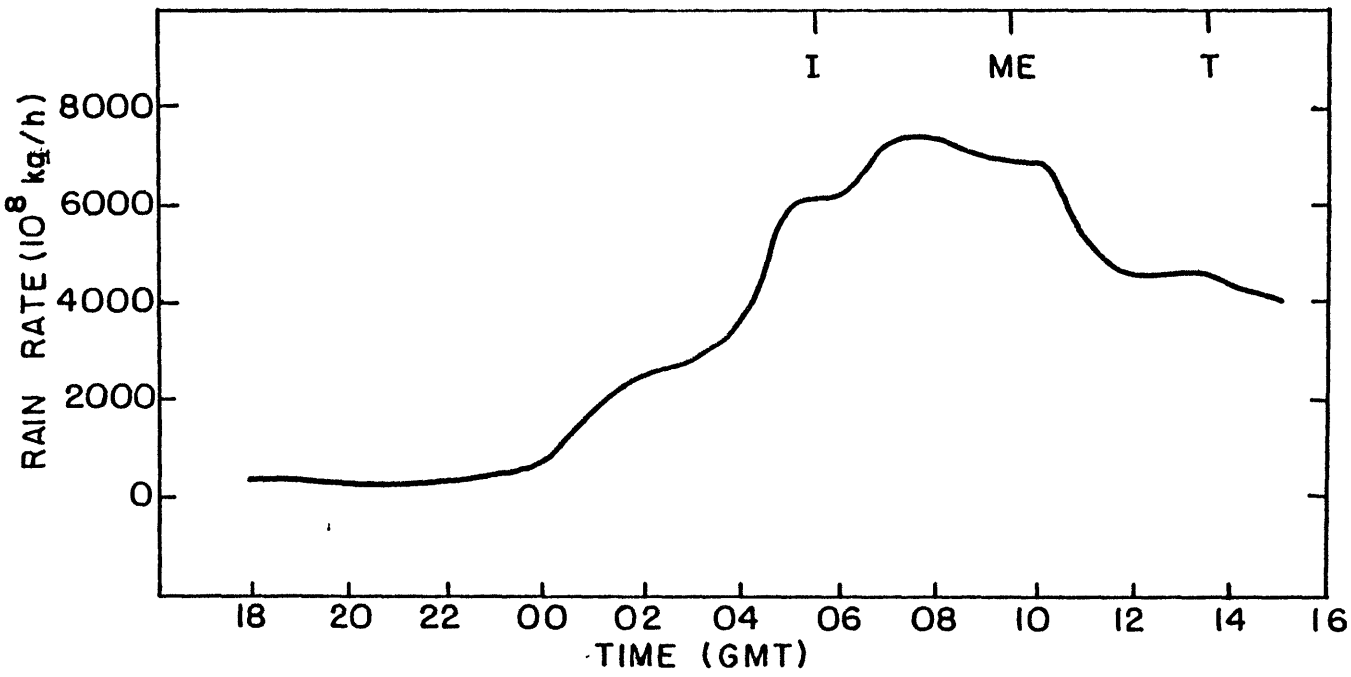
I
ME
T
RAIN RATE (10^8 kg/h)
8000
6000
4000
2000
0
18
20
22
00
02
04
06
08
10
12
14
16
TIME (GMT)

Figure 3. Total intensity[1], MCC of 19/20 May 1979(B).

[1]Intensity is computed by averaging observed intensities, therefore plotted intensity does not equal plotted rain rate divided by area unless convective correction factor,.36, is taken into account.

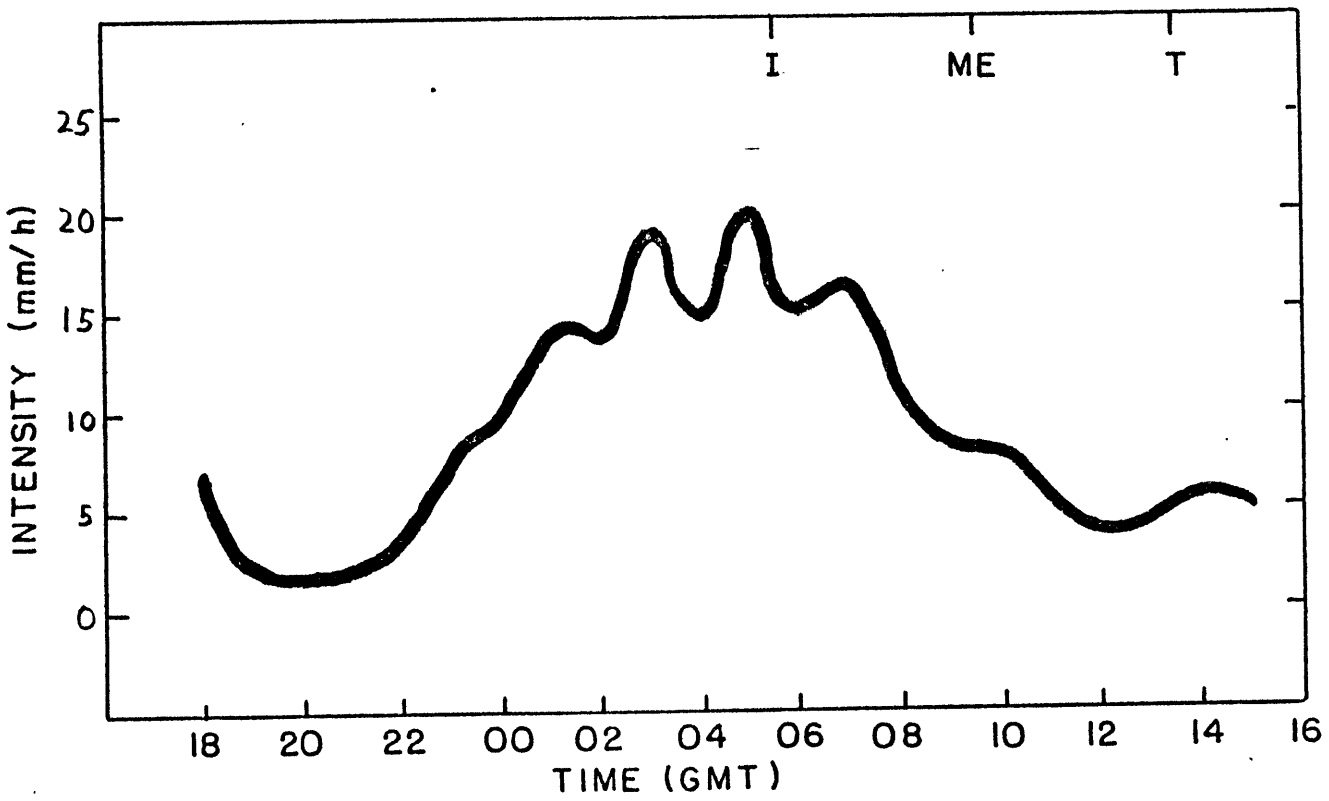
I ME T
25
20
15
10
5
0
INTENSITY (mm/h)
18 20 22 00 02 04 06 08 10 12 14 16
TIME (GMT)

Figure 4. Area of convective and stratiform rain, MCC of 19/20 May 1979(B). Convective and stratiform rain areas are denoted by dashed and solid lines, respectively.

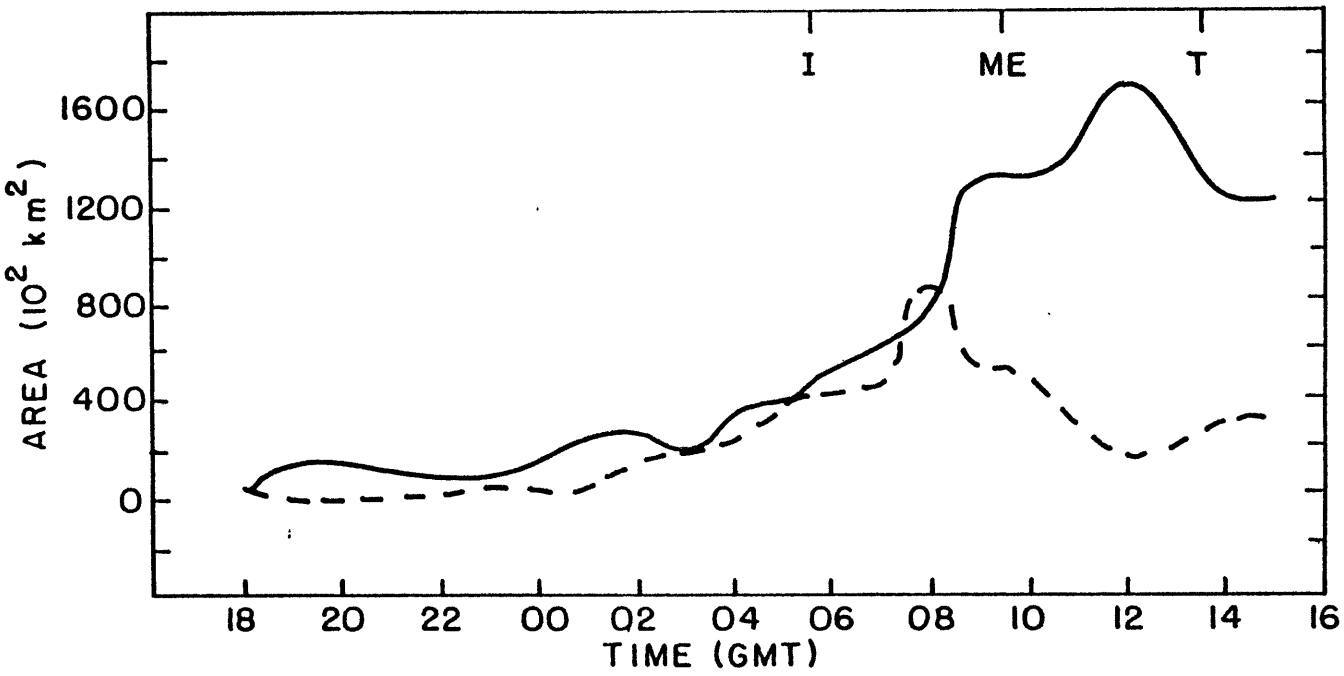
I
ME
T
1600
1200
800
400
0
AREA (10^2 km^2)
18
20
22
00
02
04
06
08
10
12
14
16
TIME (GMT)

increase in both types of rain. Small upward surges of the convective total, along with a lessening of the increase in the stratiform rain, indicates the growth of convection in stratiform areas. At about 0800 GMT a significant development occurs; the area of convection starts decreasing and the stratiform rain continues to increase. This change occurs before the cloud top reaches maximum extent and from a convective viewpoint might be considered the beginning of storm decay. With respect to processes creating stratiform rain, they do not peak until after the MCC reaches maximum cloud extent.

Fig. 5 gives an hour by hour comparison of the relative mass of rain falling in the convective and stratiform areas. The rain rate data can be roughly interpreted as latent heat release. Note the substantial domination of the convection in the early part of the MCC and the dominance of stratiform rain later. Convective then stratiform dominance is reflected in the numerical model of Keitzberg and Perkey (1977), and represents a system first dominated by convective updrafts then later by stable updrafts. Even though the stratifrom rain grows while the convection decays, some amount of convection is probably needed to keep the stratiform rain growing. This is implied by the rapid drop in the convective rain rate shown in Fig. 5 at 1200 GMT, and the peaking of the stratiform rain area growth shown in Fig 4. Some results in section 6 also emphasize this fact, that an MCC is a convectively driven system even though other mesoscale circulations become significant.

Changes in the intensity of the stratiform and convective rain is illustrated in Figs. 6 and 7. The stratiform rain undergoes a general rise in intensity, while the convective intensity shows a sharp peak then a gradual decline. For the average MCC this peak occurs in the late

Figure 5. Convective and stratiform rain rates, MCC of 19/20 May 1979(B). Convective and stratiform rain rates are denoted by dashed and solid lines, respectively.

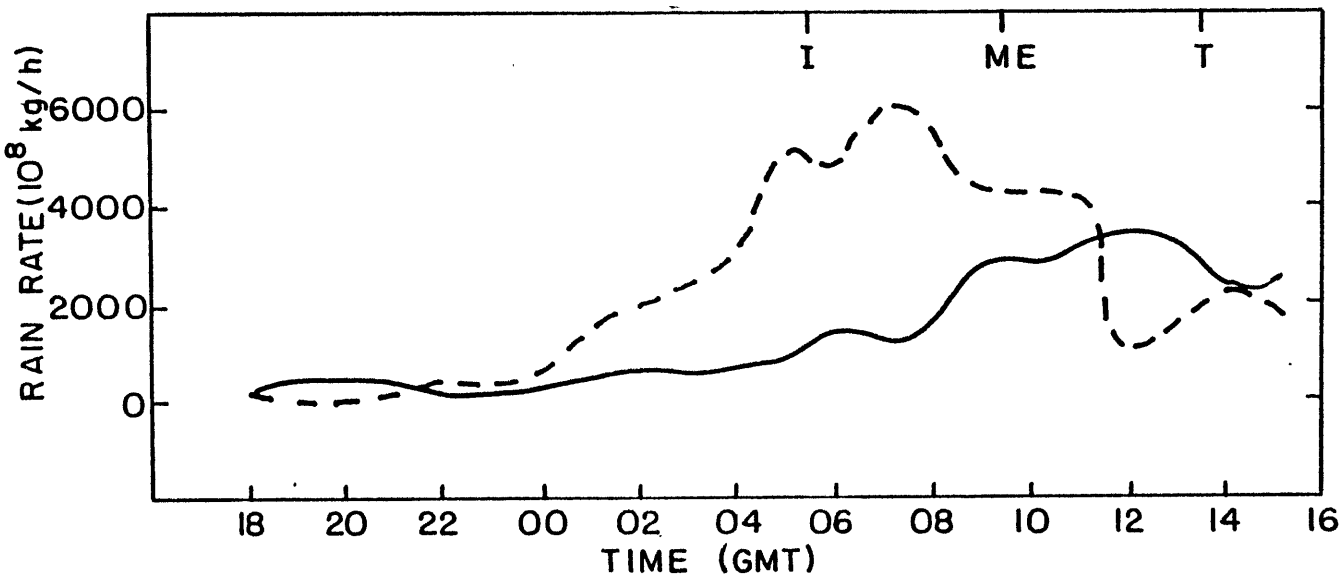
I
ME
T
RAIN RATE(10^8 kg/h)
6000
4000
2000
0
18
20
22
00
02
04
06
08
10
12
14
16
TIME (GMT)

Figure 6. Stratiform rain intensity, MCC of 19/20 May 1979(B).

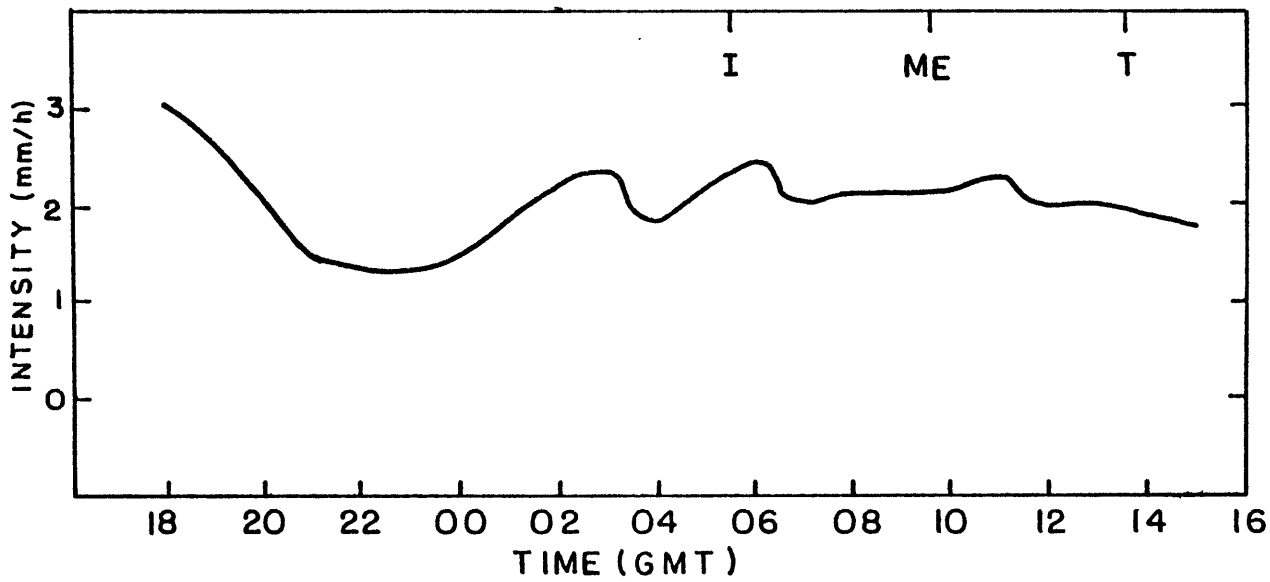
I
ME
T
INTENSITY (mm/h)
3
2
1
0
18
20
22
00
02
04
06
08
10
12
14
16
TIME (GMT)

Figure 7. Convective rain intensity, MCC of 19/20 May 1979(B).

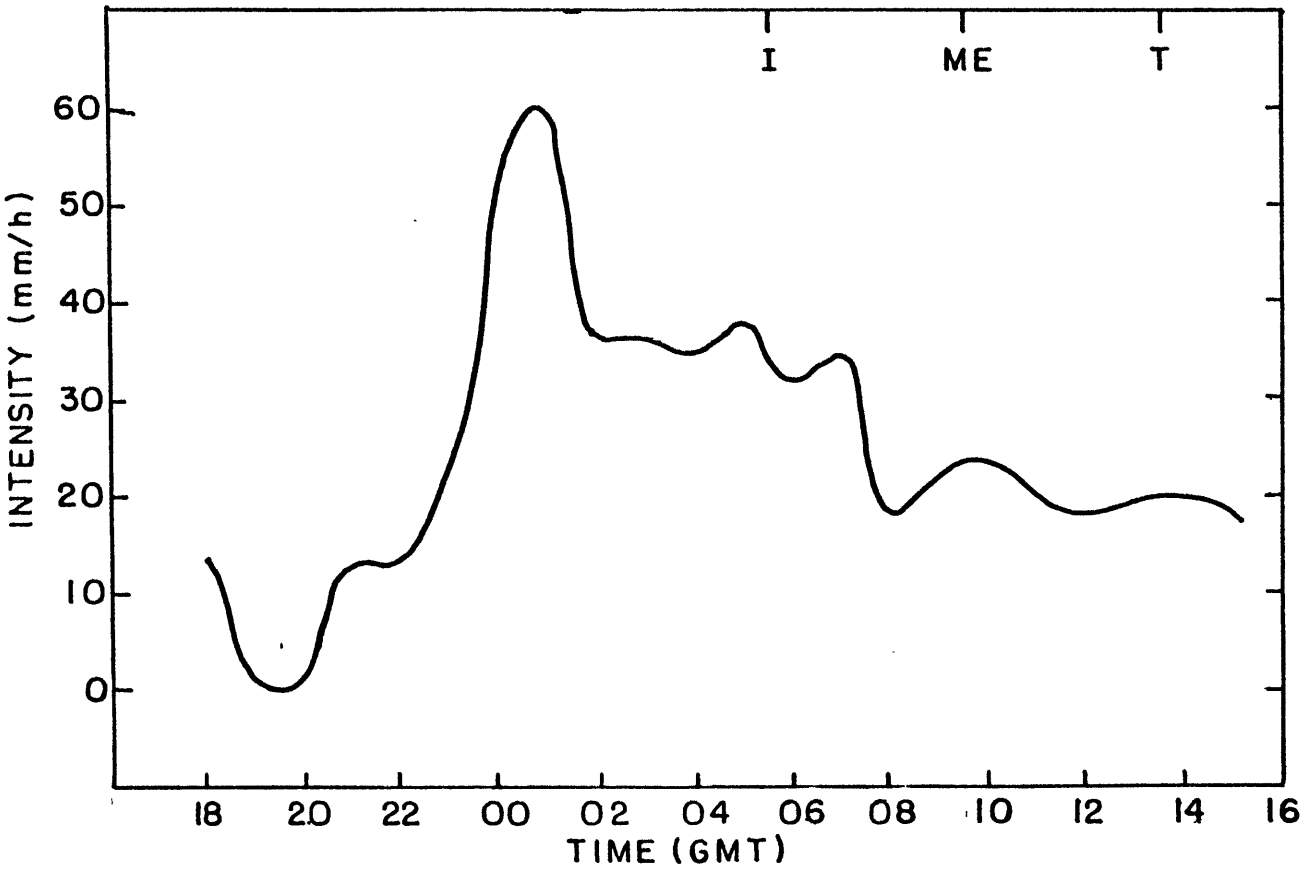
I ME T
60
50
40
30
20
10
0
INTENSITY (mm/h)
18 20 22 00 02 04 06 08 10 12 14 16
TIME (GMT)

afternoon.

After examining the radar data for a number of MCCs, it became apparent that a slightly different presentation of the convective and stratiform amounts would highlight some of the more important events. Data from the May 1979(B) case was again labeled either stratiform or convective, with only data of intensity level 2 plotted for stratiform and levels 4 to 6 for convective rain. These criteria were chosen because: a) intensity level 2 usually appeared on the radar maps in large groups and was the clearest indicator of widespread rain, and b) levels 4 to 6 would give a better indication of the vigor of the convection because they are the samples of more likely convective areas.

Examination of Figs. 8 and 9 suggest that the beginning of the stratiform rain started with the original intense convective impulse with fairly steady growth until the convection rapidly dropped off. The steep drops in the convective rain rates during the period 0800-0900 GMT and 1100 GMT with the resulting large increase in the stratiform area during the same periods indicates that the rapid increase in stratiform rain area as the convection drops off is a result of large amounts of convection decaying into stratiform rain at that time.

The observations above give only a partial picture of the behavior of precipitation in an MCC. A fuller understanding can be obtained by also observing the horizontal structure, and this will be done next.

Figure 8. Modified presentation of convective and stratiform rain areas, MCC of 19/20 May 1979(B). Convective and stratiform rain areas are denoted by dashed and solid lines, respectively.

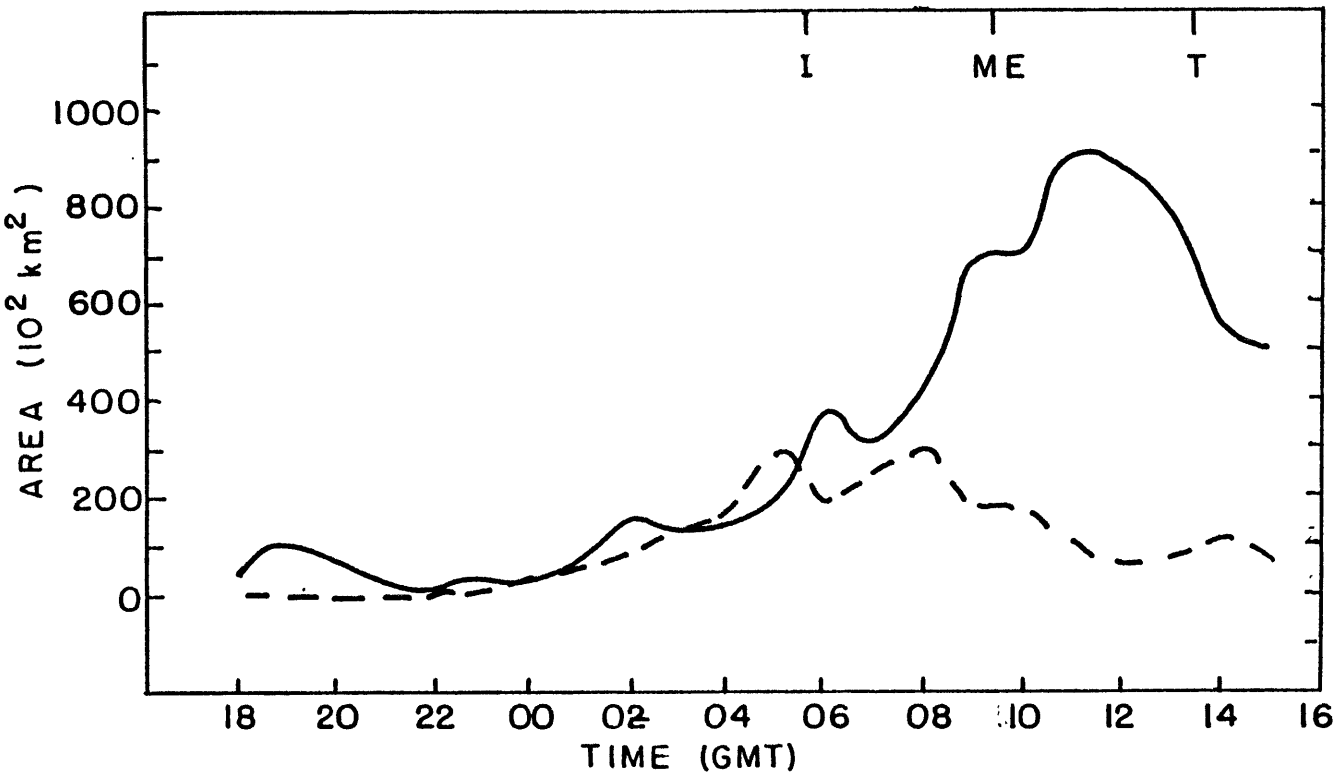
I ME T
1000
800
600
400
200
0
AREA (10^2 km^2)
18 20 22 00 02 04 06 08 10 12 14 16
TIME (GMT)

Figure 9. Modified presentation of convective and stratiform rain rates, MCC of 19/20 May 1979(B). Convective and stratiform rain rates are denoted by dashed and solid lines, respectively.

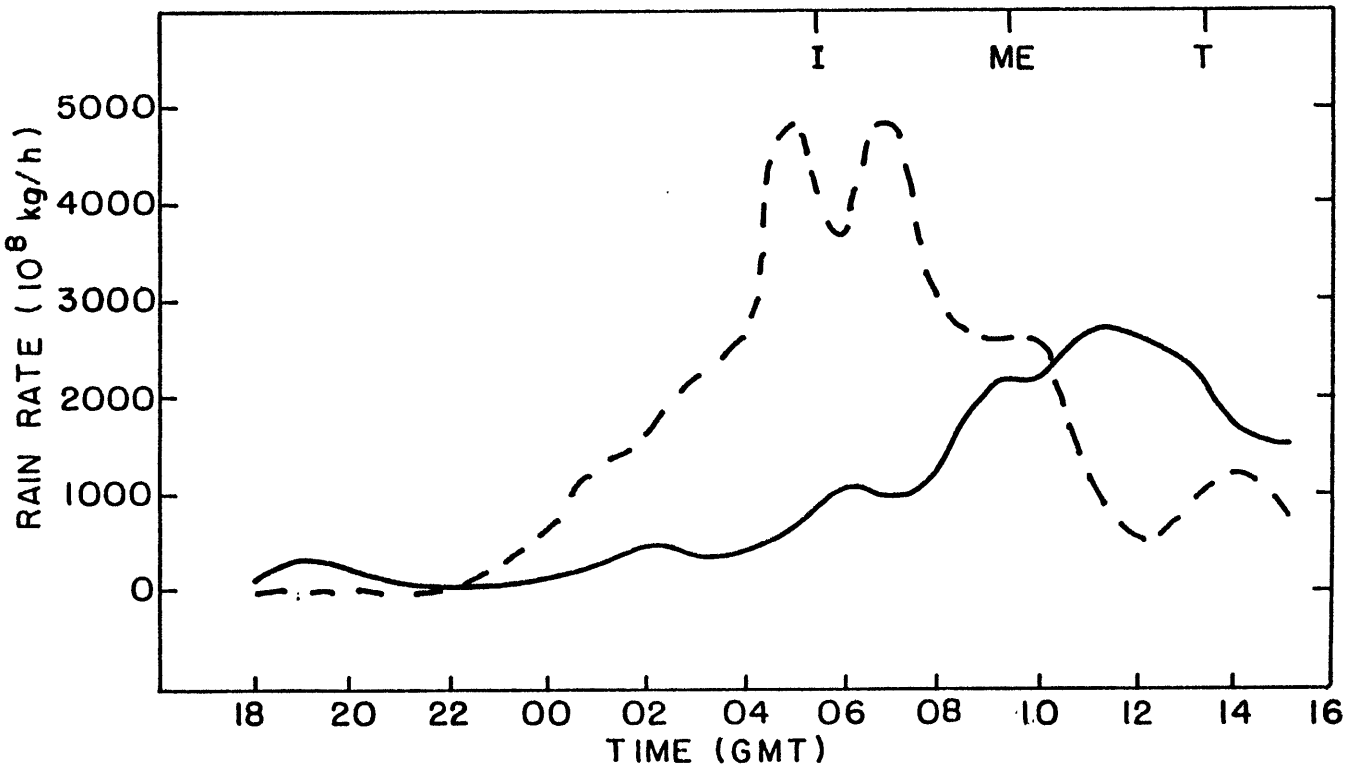
I
ME
T
5000
4000
3000
2000
1000
0
RAIN RATE (10^8 kg/h)
18
20
22
00
02
04
06
08
10
12
14
16
TIME (GMT)

5. Synoptic conditions for MCC of 19/20 May 1979(B)

At 0000 GMT, 20 May 1979 the synoptic conditions closely match the MCC genesis conditions as represented by Maddox' composite storm. The genesis region for this MCC is approximated by the circle, centered in SW Kansas, in Fig. 10. Matching surface features included a low to the west and a surface front within the genesis region. Upper air similarities are displayed in Fig. 11. The 500 mb chart shows a trough approaching from the west along with generally SW winds which closely approximate the mean tropospheric wind. A final likeness to Maddox' model is seen in the stability analysis of Fig. 12. A maximum in the analysis of lifted index is found within the genesis region with generally unstable air to the south and more stable air north.

Detailed synoptic or mesoscale analysis of the MCCs in this study was not attempted because of the inferior quality of the available surface and upper air data and the emphasis on the radar derived cycles and structures. By showing the similarities between the May 1979 MCC and Maddox' composite model it is assumed other aspects of the composite model can be used and its interpretation tested for compatability with the results of this study. Other observations and models of similar mesoscale systems will be used when they appear to supply explanations of the radar derived behavior which can not be found completely in the data available for this study.

Figure 10. Surface map for 20 May 1979, 0000 GMT. Solid lines are sea level isobars. Circle approximates area of Maddox' genesis region.

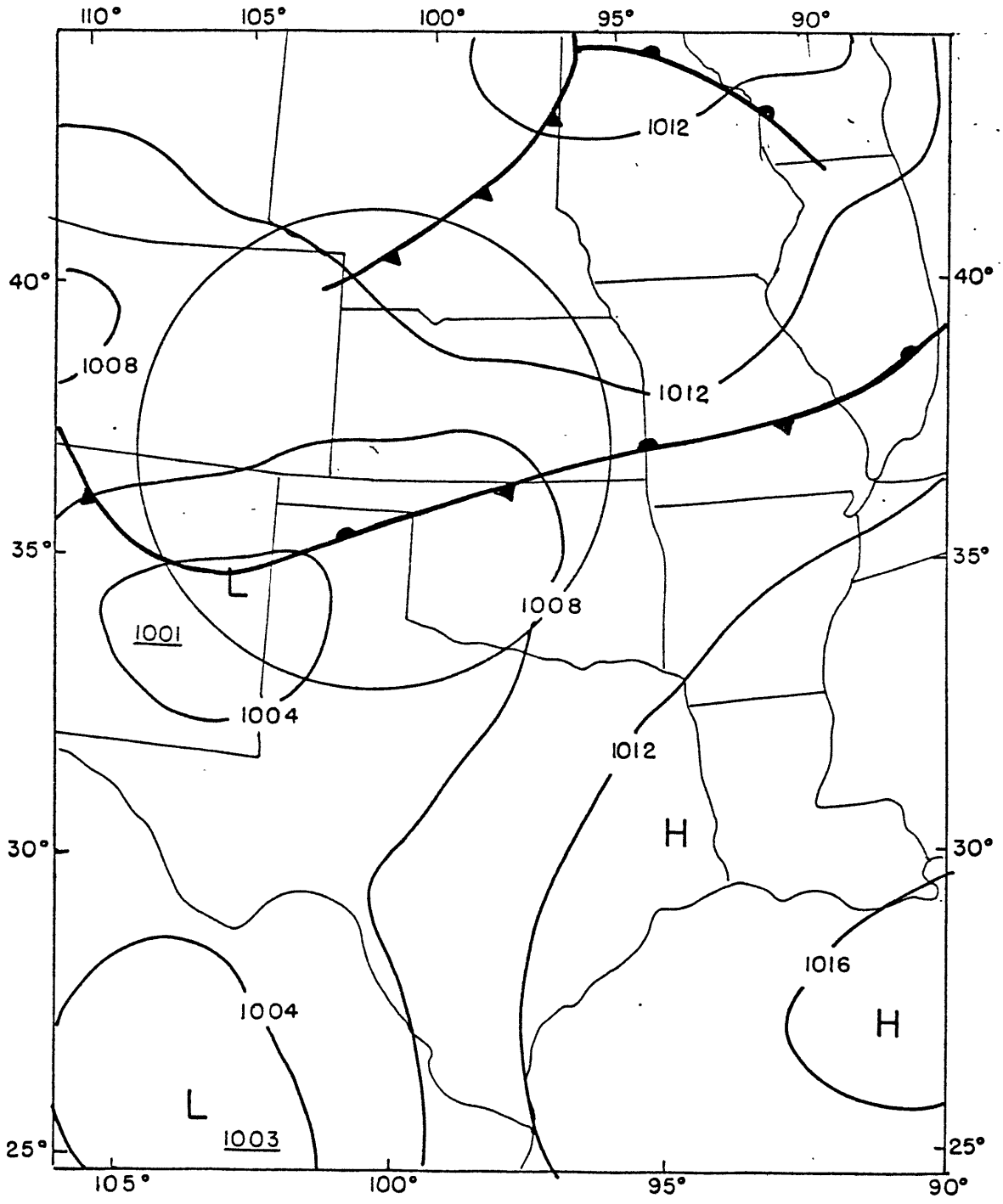
110°
105°
100°
95°
90°
40°
35°
30°
25°
1012
1008
1012
L
1001
1008
1004
1012
H
1016
H
1004
L
1003

Figure 11. Upper air chart, 500 mb, 20 May 1979, 0000 GMT. Solid lines are heights in 60 dam intervals and dashed lines are isotherms.

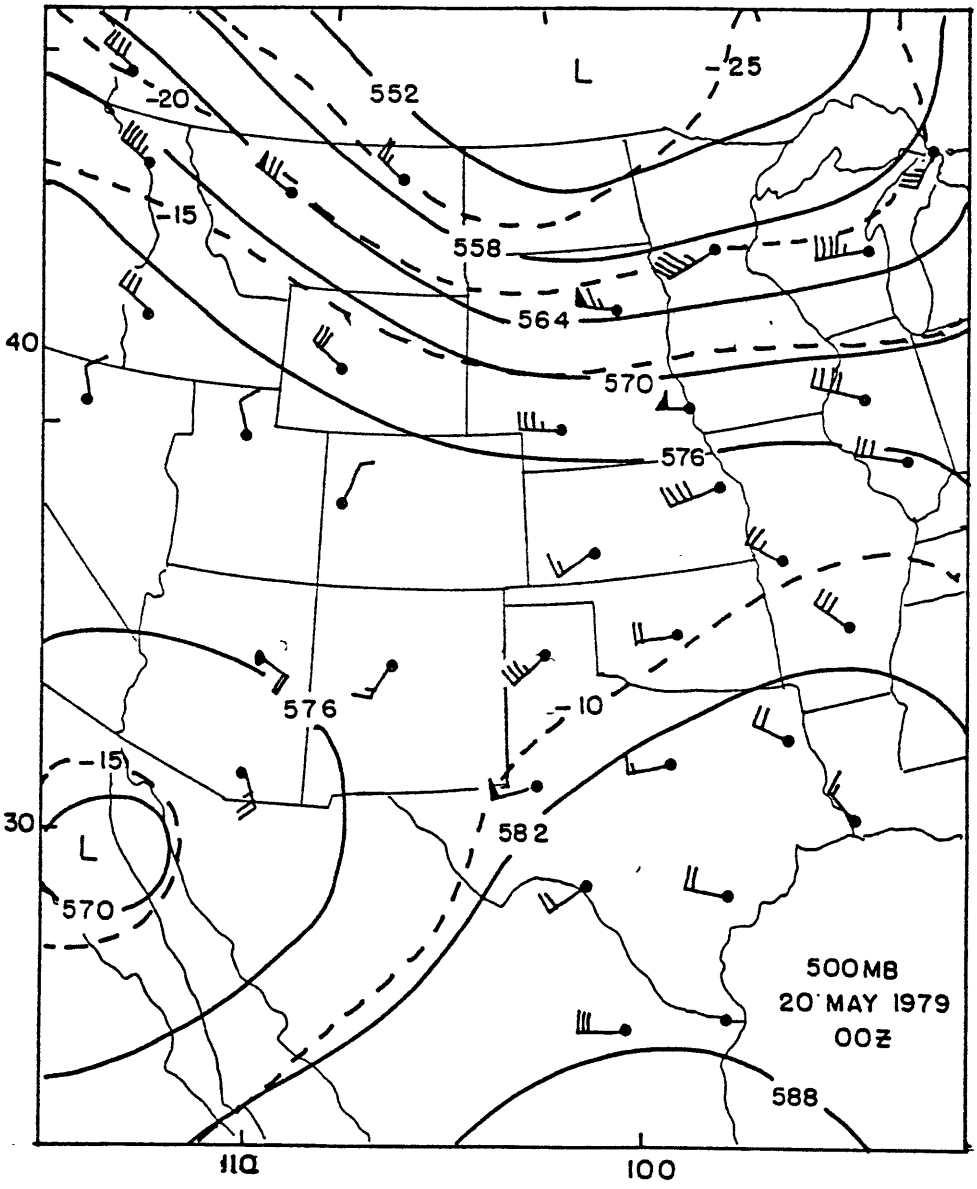
L
-25
-20
552
-15
558
564
40
570
576
576
-10
-15
30
L
582
570
500MB
20 MAY 1979
00Z
588
110
100

Figure 12. Stability analysis, lifted index, 20 May 1979, 0000 GMT.

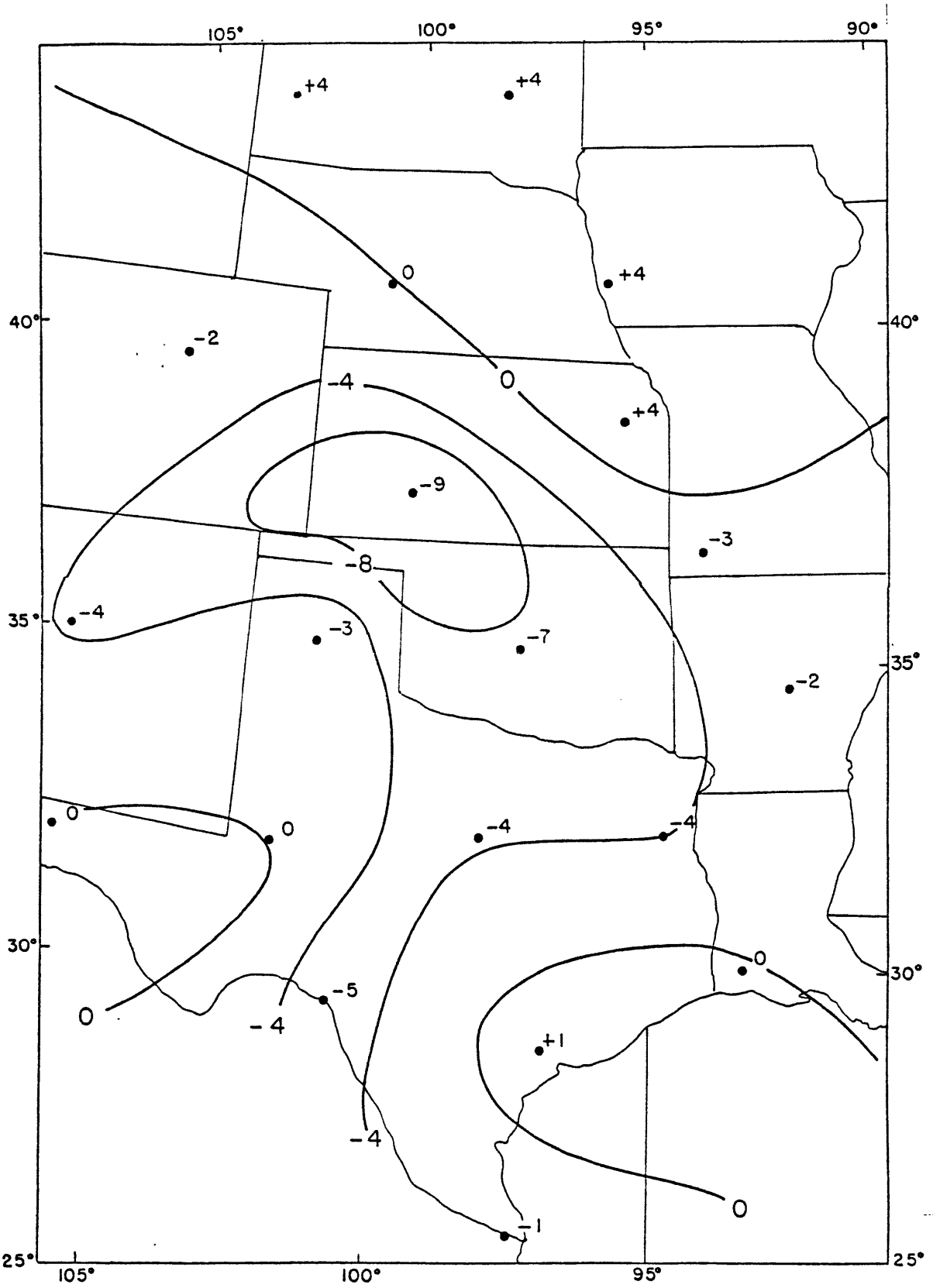
105°
100°
95°
90°
40°
35°
30°
25°
+4
+4
0
+4
-2
0
-4
+4
-9
-3
-8
-4
-3
-7
-2
0
0
-4
-4
0
-5
-4
+1
-4
0
-1

6. Horizontal precipitation structures

The horizontal structures described in this section were generally observed in most of the analyzed cases. Radar data for each MCC was taken by a number of stations; approximately ten stations were used during the life of each storm. Since observation data was collected in a PPI mode, and not reconstructed into constant altitude displays, it was not possible to determine at what altitude the data for a particular grid box was taken. Concern for this height variability is eased by the knowledge that standardized observing practices include the use of low elevation angles. With this restriction in mind, it is concluded that most data was taken below the freezing level in rain.

Fig. 13 is the combined radar map for 20 May 1979, 0135 GMT. The skewing of the map towards the northeast is caused by the application of the LFM grid to the curved globe. Numbers 1 to 6 represent intensity levels and rainfall rates as described in section 2. Either the symbol 7 or M indicate radar station location. The symbol 7 indicates available station reports; the symbol M indicates missing reports. When data is available at a station location grid, the data is plotted. Dots are grid box locations while stars indicate both grid boxes and state boundaries. Since there is another MCC and other rain areas on this map, the data included in the storm of interest is heavily outlined. All data was available along the track of the storm.

The time 0135 GMT corresponds with the peak of convective intensity (See Fig 7). Notice the clump of convection in the SW corner of the storm. This is the side from which the mean tropospheric flow is coming. Another area of convection is downwind of the first, and located near

Figure 13. Radar map, 20 May 1979, 0135 GMT. Numbers 1 to 6 indicate intensity as described in Table 1, seven means data was available from the station and plotted, while M indicates missing data. Plotted data overides 7s. Data considered part of the MCC of interest is enclosed by a heavy outline. The area within the heavy outline roughly corresponds to the area of cloud top with temperatures less than -32° C for this MCC. Areas of intensity level 2 and above are lightly outlined, and areas of 3 and above are outlined and shaded.

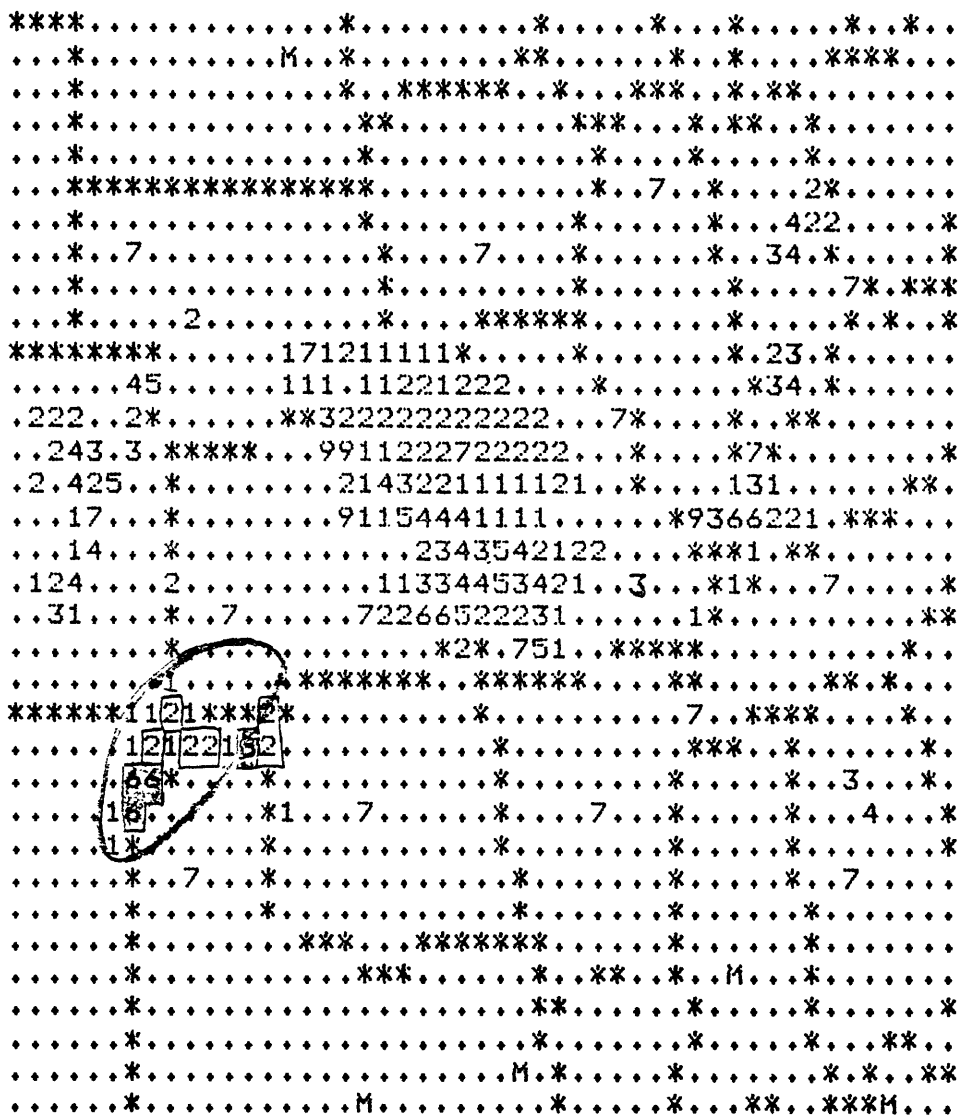

the right edge of the cirrus cloud which is streaming NE from the convection to the southwest. This dual-convection structure was often observed in other MCCs and tends to persist. As the convective growing stage continues, the MCC begins to take on characteristics of a tropical squall line as observed by Houze (1977), i.e., a line of convection with a trailing cloud shield. In the case of the MCC, the main convection area is trying to propagate into the mean flow (Figs. 14 and 15). More similarities between the tropical and mid-latitude mesoscale systems will be presented in later sections.

Shortly after the maximum convective rain rate was reached (see Fig. 5) drastic structural changes began. First, as shown in Fig. 16, the convective freeregion in the center of the MCC appeared to fill with convection, but because of the large grid size, it is not clear how this happened. Other cases, however, showed this same behavior. Next (see Fig.17) a line of convection (marked by the dashed line) formed on the SE side of the storm and the convection on the W side was significantly reduced. The convective line on the SE side of the MCC was roughly aligned with the mean wind and is probably the same as the linear features observed by Maddox (1981).

By 1235 GMT, as seen in Fig. 18, it appears that all convection along the west side of the MCC has ceased. The stratiform rain reached its peak (Fig. 4) and the line on the south side of the storm grew southward and moved east.

On the next map, (Fig. 19) 1335 GMT, it becomes apparent how important the convection on the west side of the storm was in the maintenance of the stratiform rain. With the convection gone, the stratiform rain was quickly pushed to the NE by the wind, where it decayed.

Figure 14. Radar map, 20 May 1979, 0535 GMT. Details similar to fig. 13.

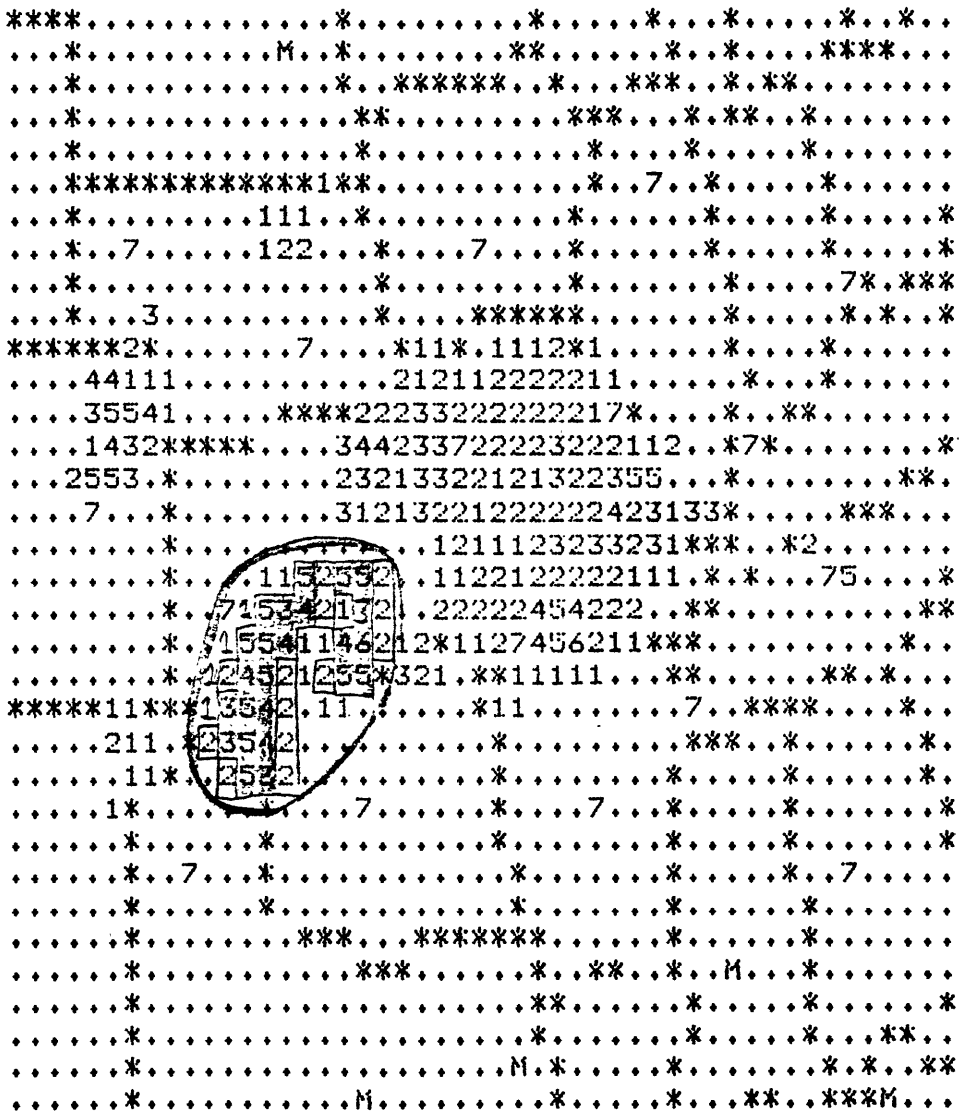

Figure. 15. Infrared satellite picture, 20 May 1979, 0530 GMT. Enhanced areas indicate cloud top temperatures less than -32° C. States overlay is slightly offset.

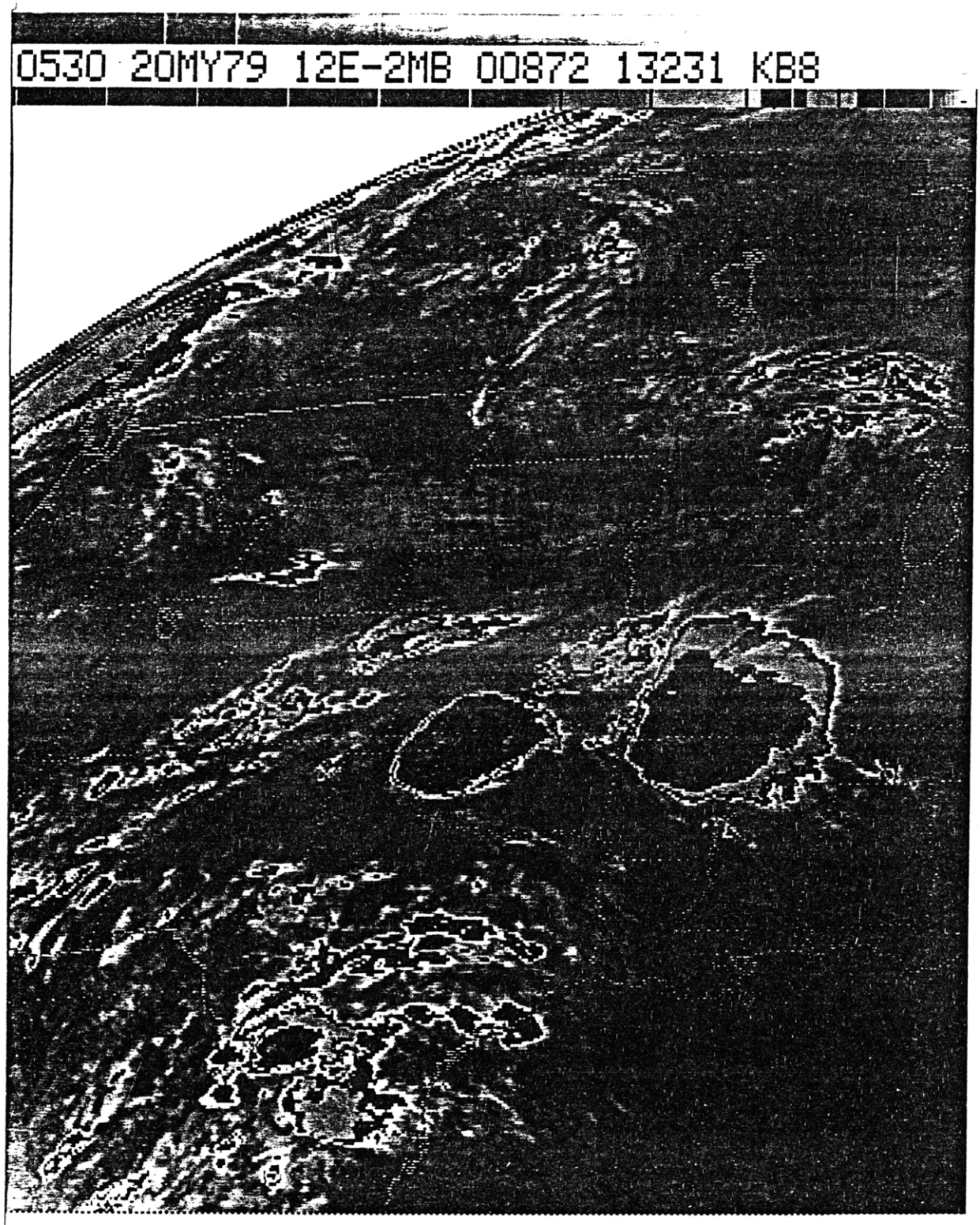
0530 20MY79 12E-2MB 00872 13231 KB8

Figure 16. Radar map, 20 May 1979, 0835 GMT. Details similar to fig. 13.

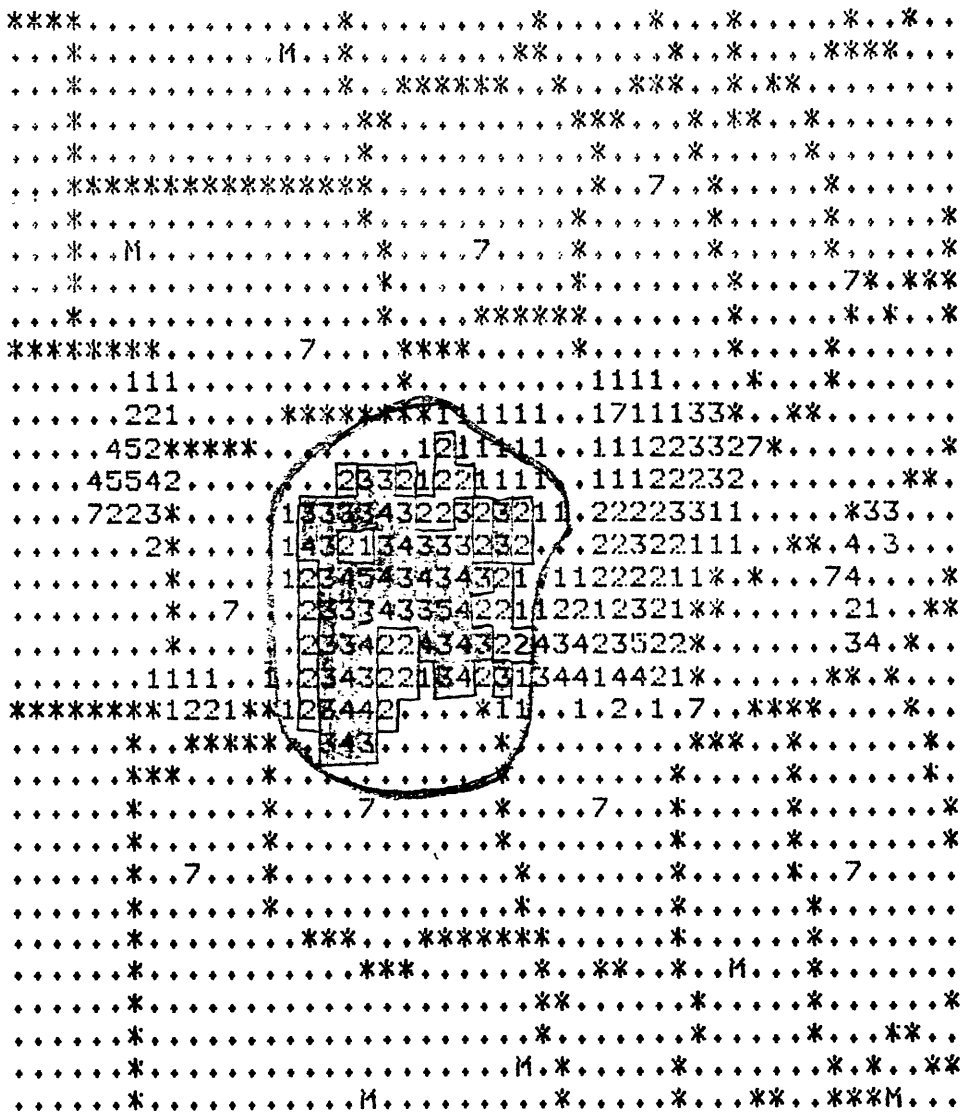

Figure 17. Radar map, 20 May 1979, 0935 GMT. Details similar to fig. 13.

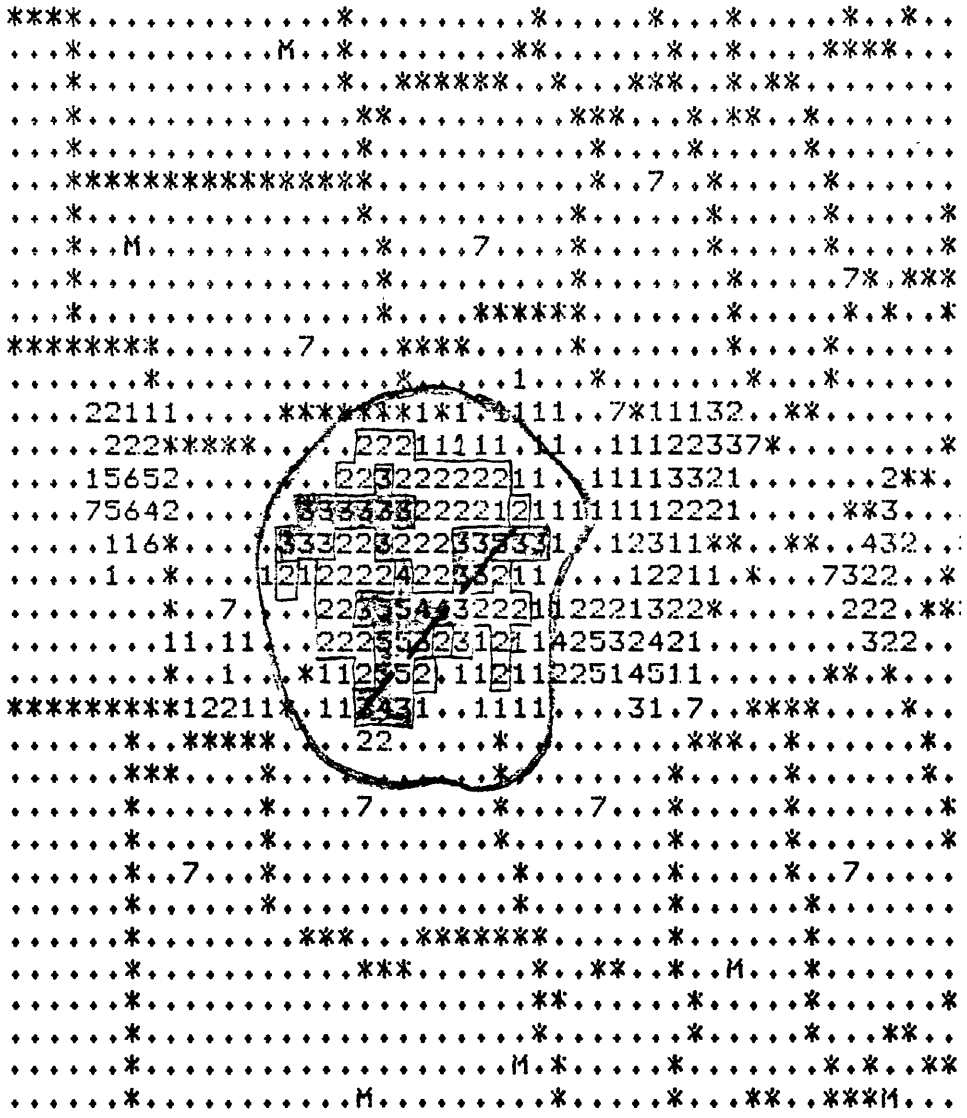

Figure 18. Radar map, 20 May 1979, 1235 GMT. Details similar to fig. 13.

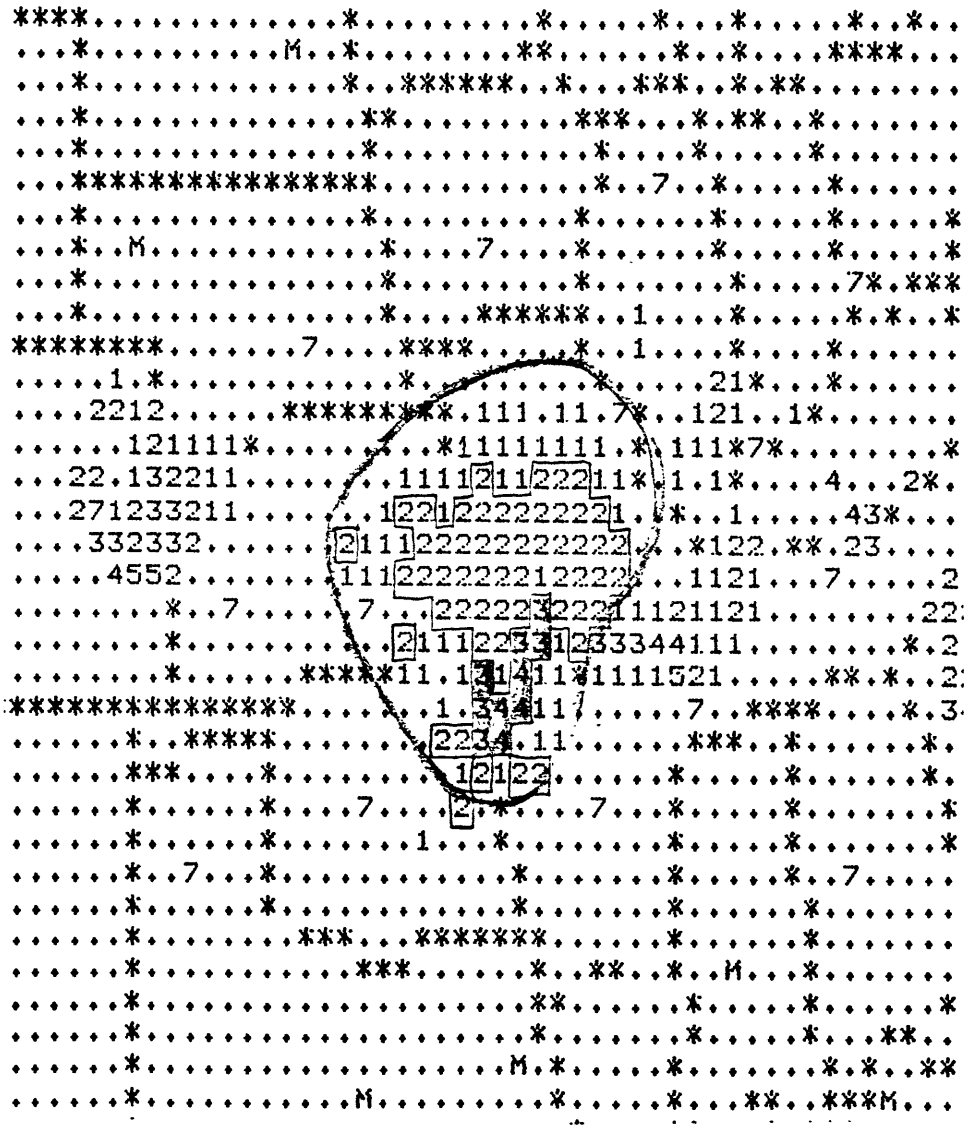

Figure 19. Radar map, 20 May 1979, 1335 GMT. Details similar to fig. 13.

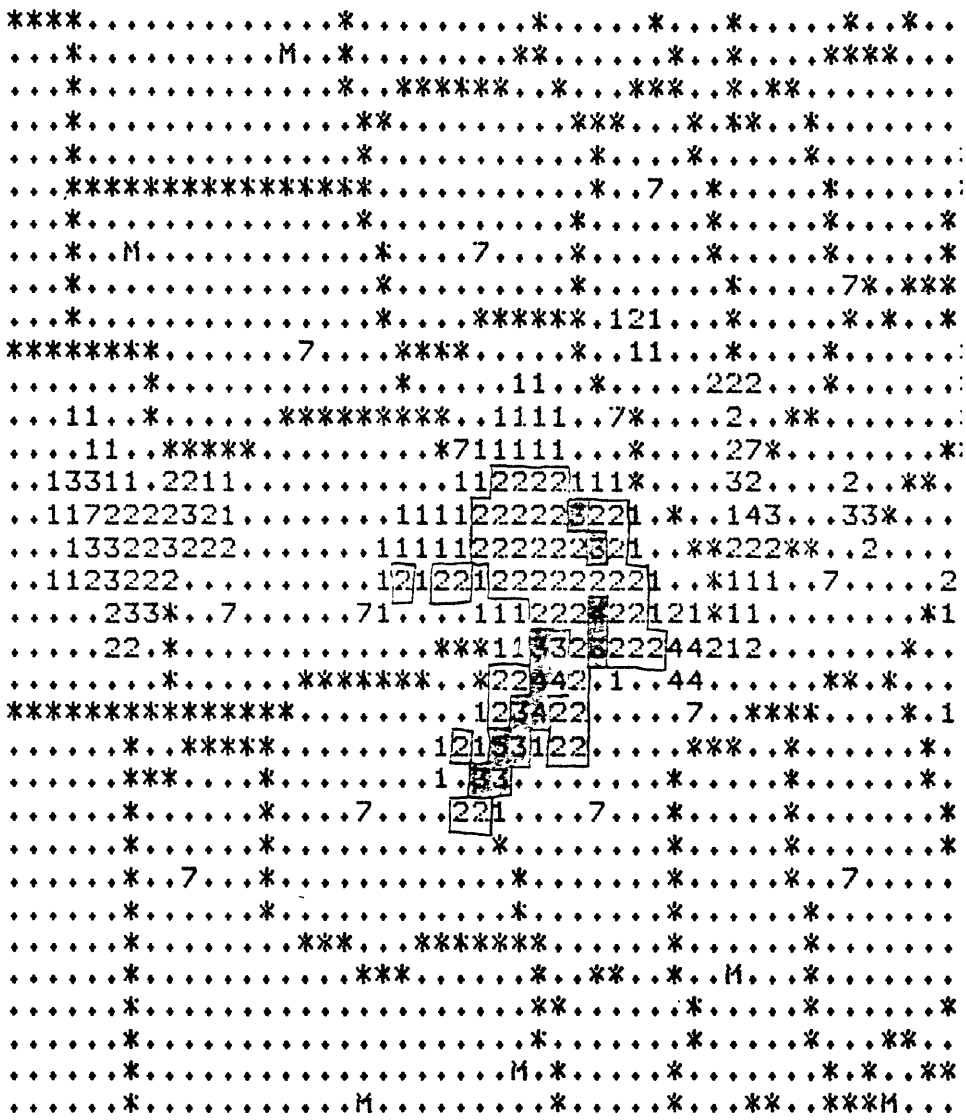

character of a weak midlatitude squall line. The line is roughly aligned with the mean wind, slightly bulged, and moving approximately perpendicular to its long axis (Fig. 20). This final stage was frequently observed, with the convection in each case developing to different degrees of vigor.

Figure 20. Radar map, 20 May 1979, 1535 GMT. Details similar to fig. 13.

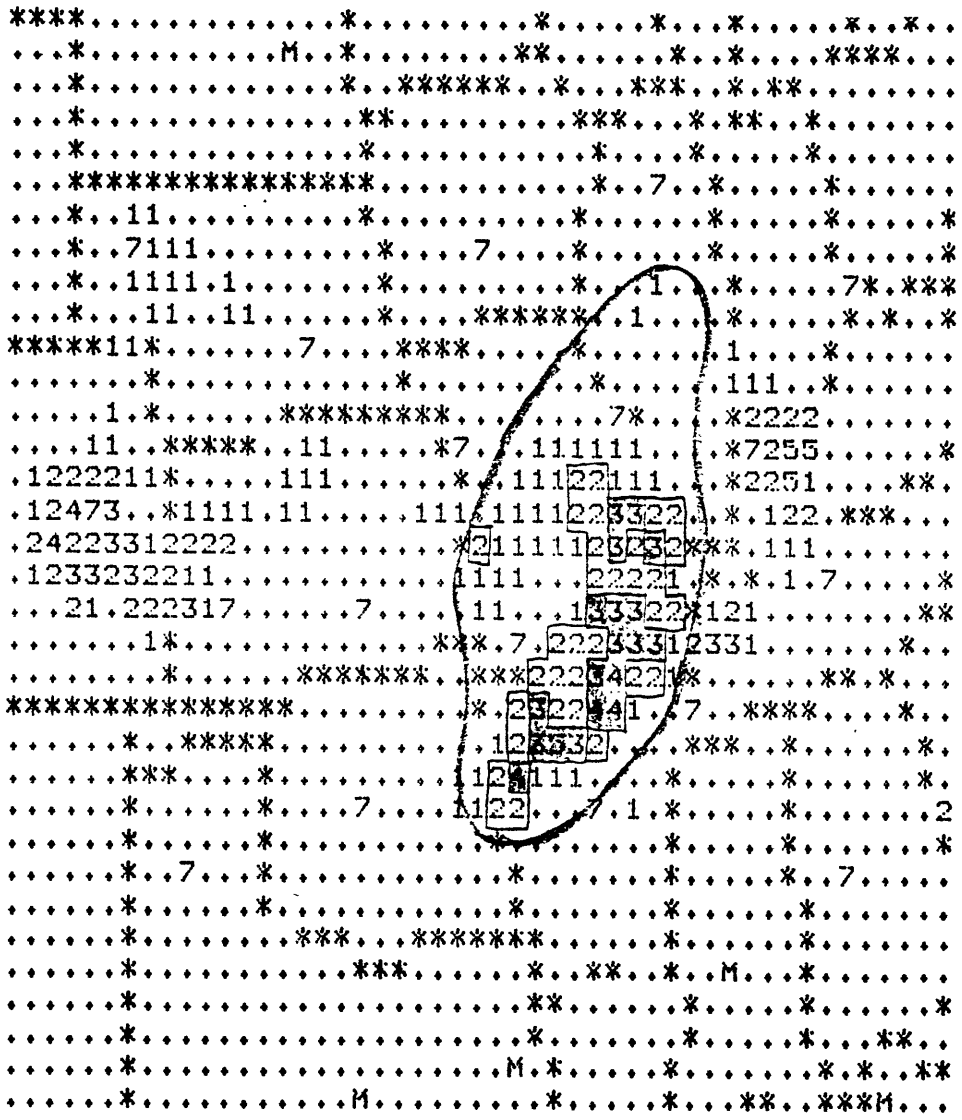

7. Evidence of the significance of mesolow aloft

One simple model of an MCC would consist of three parts-- early phase (tropical squall line-like), transition phase, and late phase (midlatitude squall line-like). The question arises -- why does an MCC change from one type of system to another? Part of the answer can be found in the composite model of an MCC constructed by Maddox (1981).

In the composite model of a mature MCC, Maddox diagnosed a strong relative mesolow which forms above the rain-induced surface mesohigh (Fig. 21). Evidence for this low can not usually be seen in the upper air patterns, because it is too small; nor in the surface fields, because these fields are dominated by the mesohighs. Examination of the surface pressure and wind for the case presented in this paper, however, does suggest the presence of a surface low in approximately a position that could help explain the late phase line, and supplies indirect evidence for the mesolow aloft (see fig. 22). The surface low's position corresponds to the northeast edge of the late phase convective line. A better example of the relationship between the surface mesolow and the late phase convective line was found in the MCC of 26/27 August 1982. Figs. 23, 24, and 25 show the satellite picture, radar map, and surface chart, respectively, for times at or near 0600 GMT.

The large cloud area resulted from the nearly simultaneous growth of three MCCs, with the one on the right being of most interest because it became very large and clearly exhibited the formation of a mesolow. The radar map shows a transitional signature for the large area of convection on the rightmost MCC. The surface map indicates a low pressure trough lying across southern Indiana and Illinois.

Figure 21. Relative wind flow at 700 mb from Maddox' (1981) composite model.

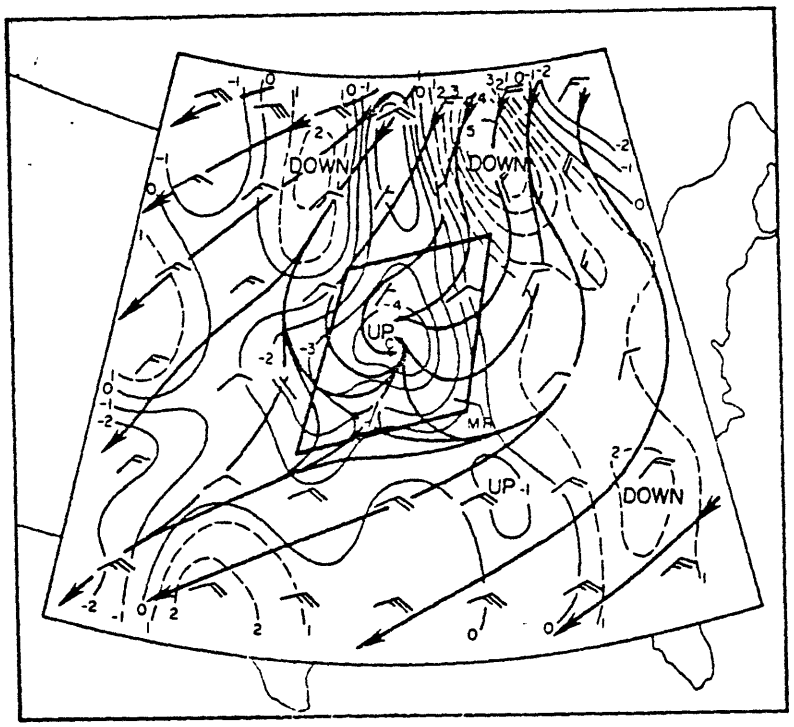

700 mb relative flow at the time of the MCC. Streamlines are shown with relative winds (full barb = 10 kt or about 5 m/s) plotted at every other grid point. Contours of omega in microbar/s (light solid and dashed lines) are shown for the total flow.

Figure 22. Surface map, 20 May 1979, 1200 GMT from Maddox (1981) except for low which was added.

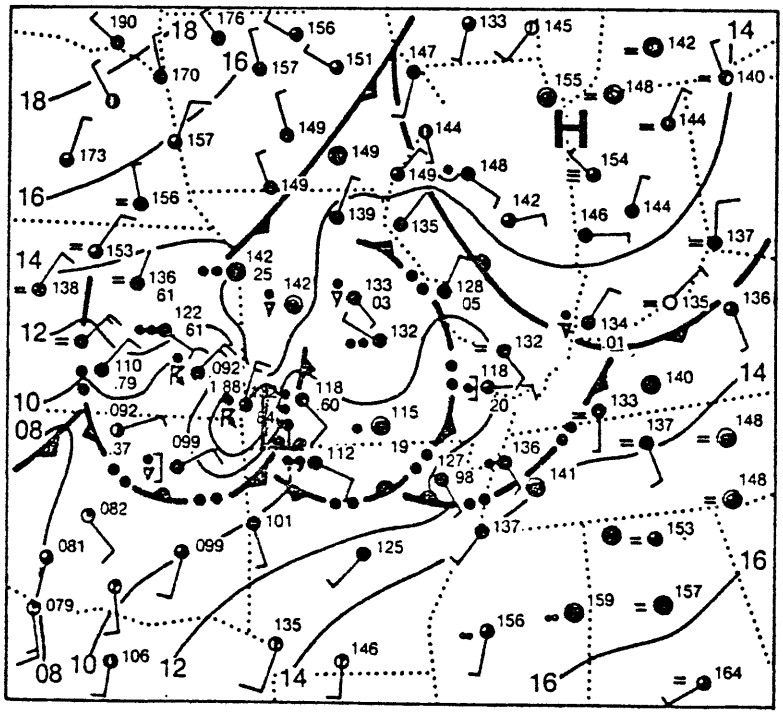

Surface analysis for 1200 GMT 20 May 1979. Surface features are indicated, along with 2 mb isobars. Winds are in kt (full barb = 10 kt or $\sim$5 m s^{-1}) and squall symbols with frontal barbs indicate positions and movements of cold air outflow boundaries. Six hour precipitation amounts, in inches, are also shown.

Figure 23. Infrared satellite picture, 27 August 1982, 0600 GMT. Enhanced areas indicate cloud top temperatures less than -32° C.

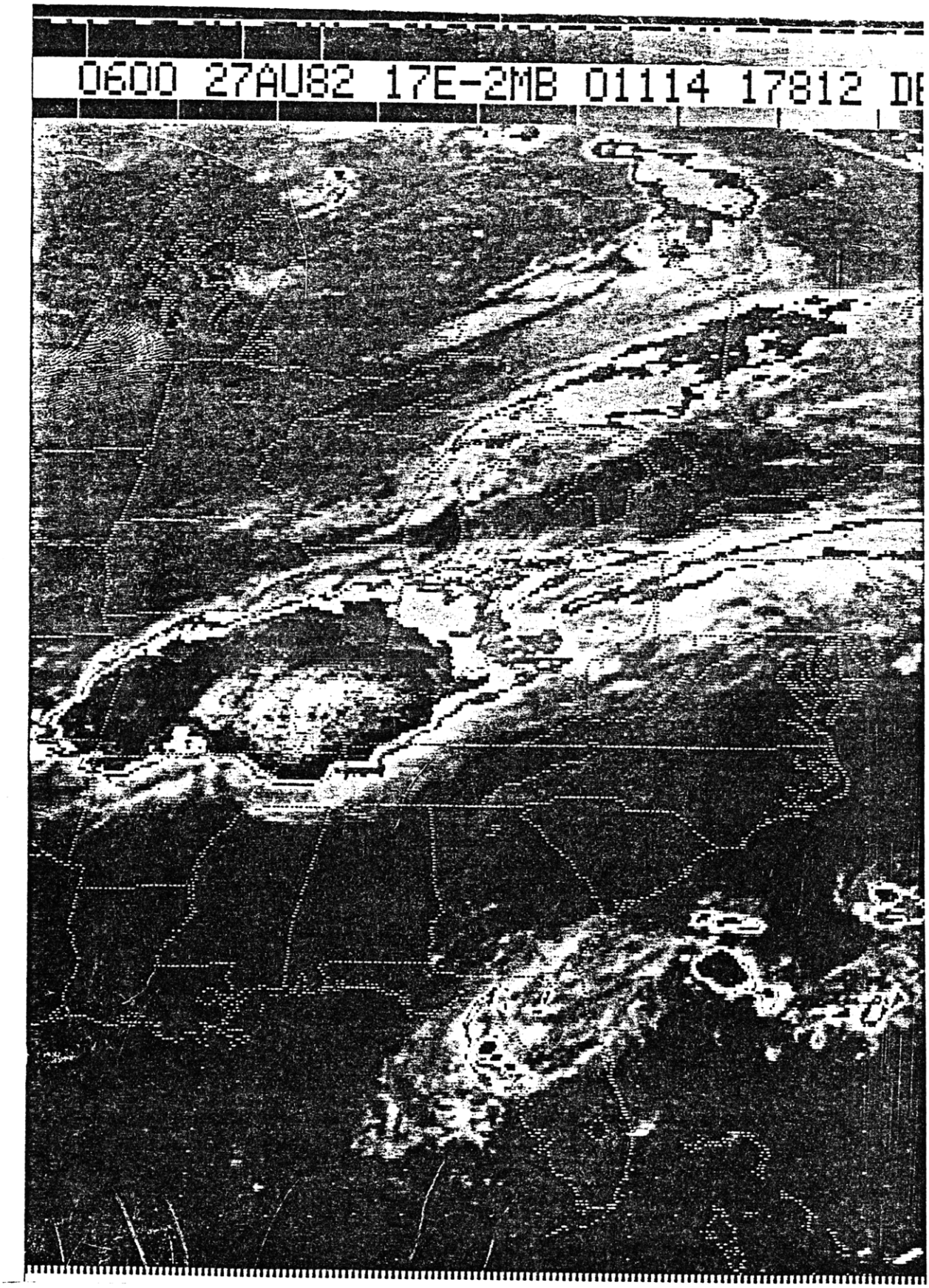
0600 27AU82 17E-2MB 01114 17812 DI

Figure 24. Radar map, 27 August 1982, 0635 GMT. Details similar to fig. 13.

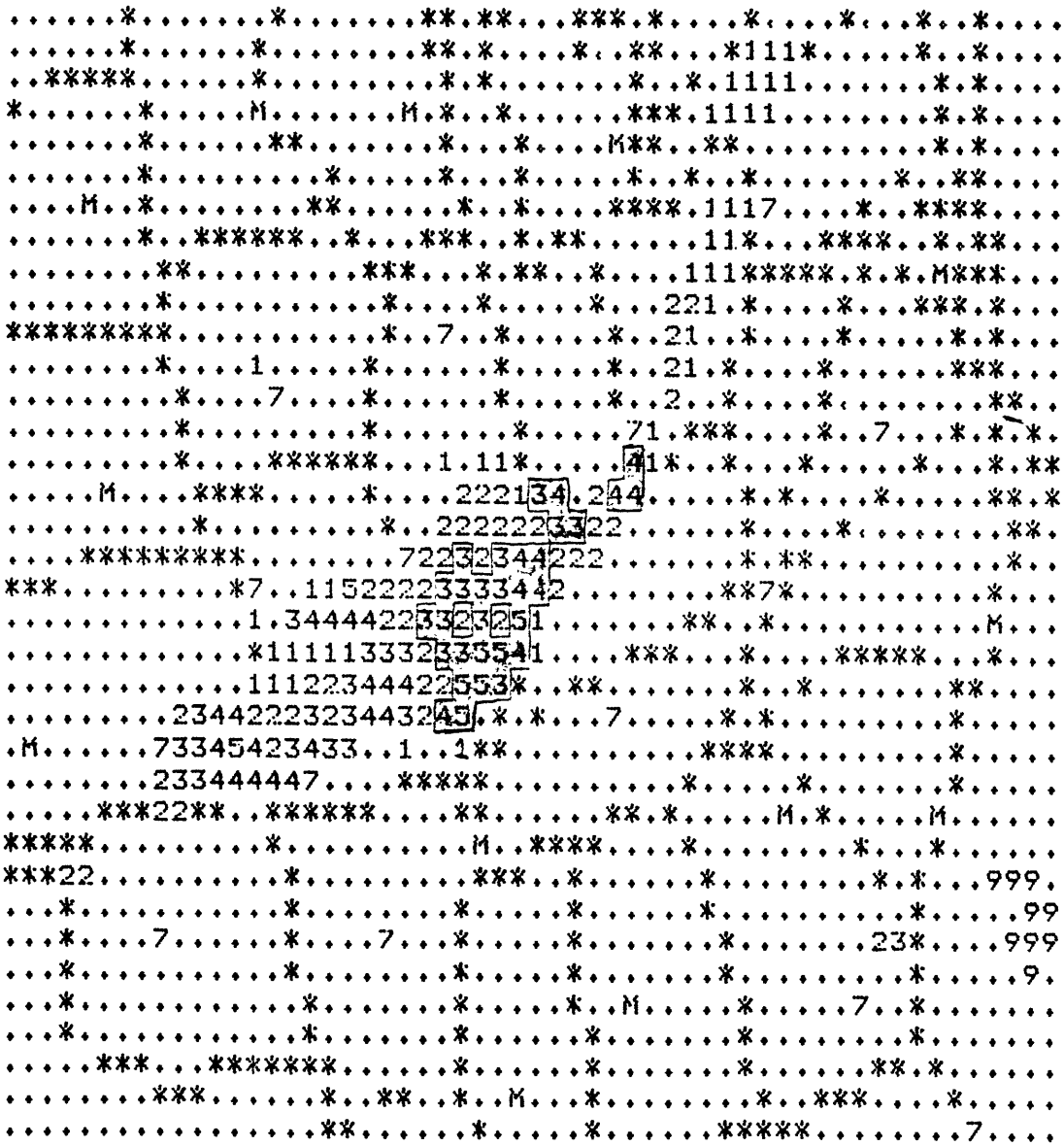

Figure 25. Surface map, 27 August 1982, 0600 GMT. Solid lines are sea level isobars.

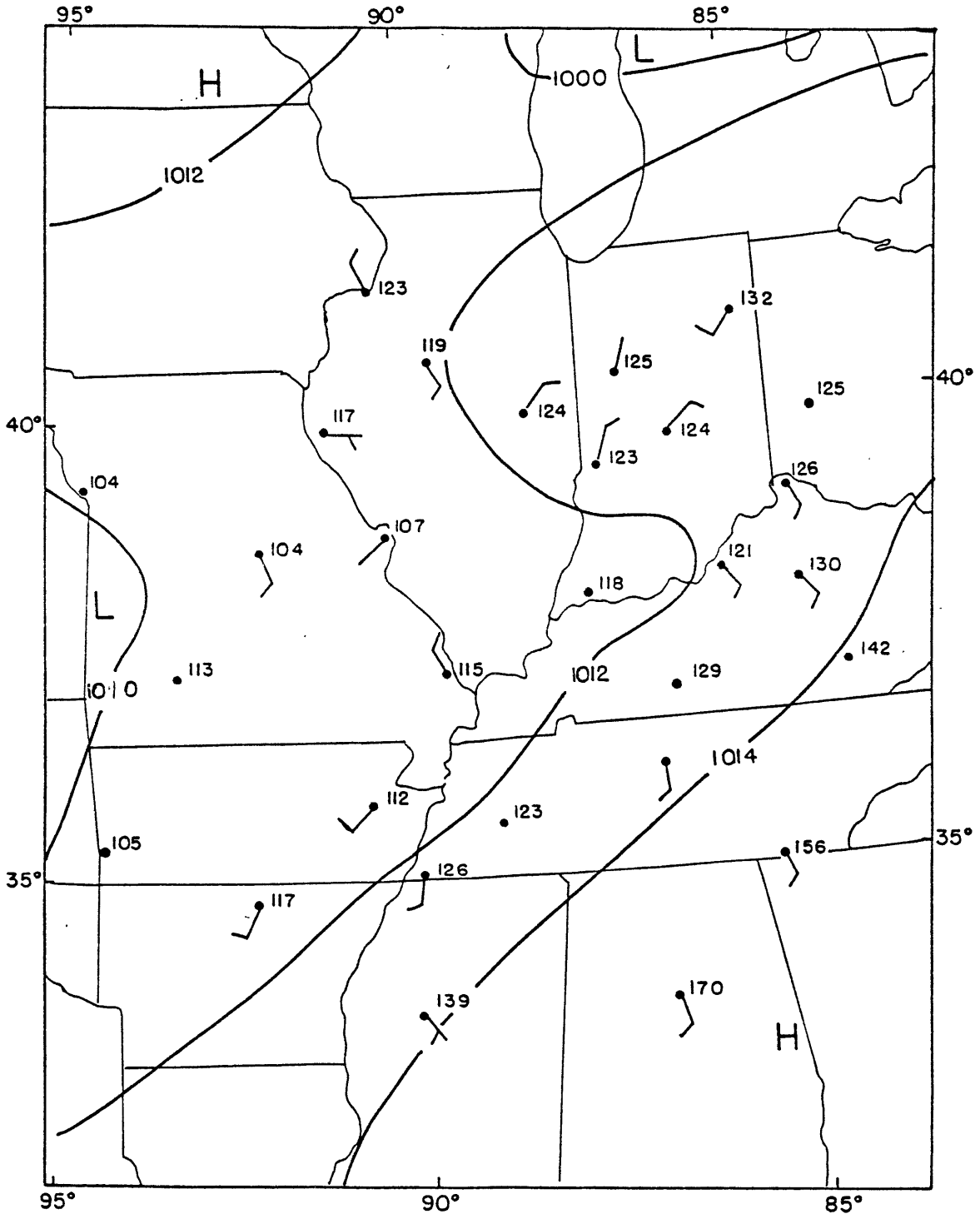
95°
90°
85°
40°
35°
H
L
1000
1012
1010
1014
123
132
119
125
124
117
104
107
126
121
130
118
113
115
129
142
112
105
156
170
139

By 0900 GMT the MCC has passed maximum cloud extent and is showing significant changes of structure. A bulge is appearing in the cloud shield on the southern side of the MCC (Fig. 26) which corresponds with the convective line on the radar map (Fig. 27), and a large mesolow has developed on the border between Indiana and Kentucky (Fig. 28). The position of the low appears to be on the north edge of the convective line, as it was in the previous case.

A final glimpse at the behavior of this MCC is given for 1200 GMT in Figs. 29, 30, and 31. At this time the convective line was weakened substantially, but a new center of organized cloud and rain area has appeared which grew through the eastern third of the MCC cloud shield. This rain is located ahead of the low in an area of expected uplift. By tracking movement of the center of the new cloud mass it was revealed that the associated low was moving east at a speed of 45 kt during the period 1000-1400 GMT, a direction and speed which was observed in the windfield of the atmospheric layer from 500-300 mb. This same behavior, the appearance of a fast moving cloud mass and rain area on the lee side of a decaying MCC, was also observed in an MCC two days before. The MCC occurring on 25 August 1982 was in the same geographic location with similar environmental flow.

An explanation of the latter August 1982 MCC behavior can only be speculated at this time. Area measurements were made of the cloud top colder than approximately -65°C. At 0800 GMT, the area measured 100,000 km^2, and by 1000 GMT, it had shrunk to nearly zero. The rapid warming of the cloud top is probably indicative of a rapid collapse of the cloud air. Widespread warming of the cloud top continued after 1000 GMT, and this warming period corresponds to the appearance of the separate cloud mass on

Figure 26. Infrared satellite picture, 27 August 1982, 0900 GMT. Enhanced areas represent cloud top temperatures less than -32° C.

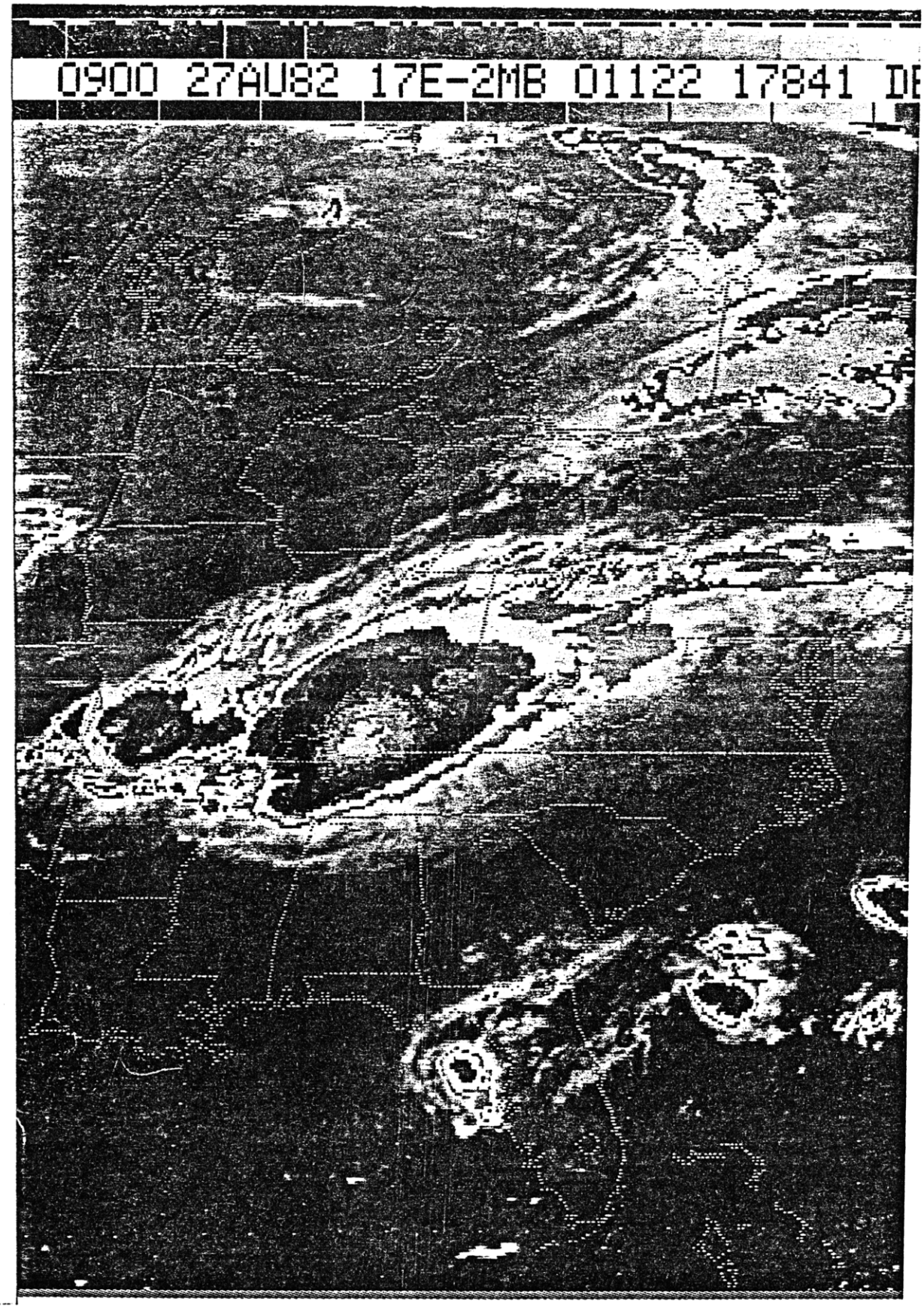
0900 27AU82 17E-2MB 01122 17841 DE

Figure 27. Radar map, 27 August 1982, 0935 GMT. Details similar to fig. 13.

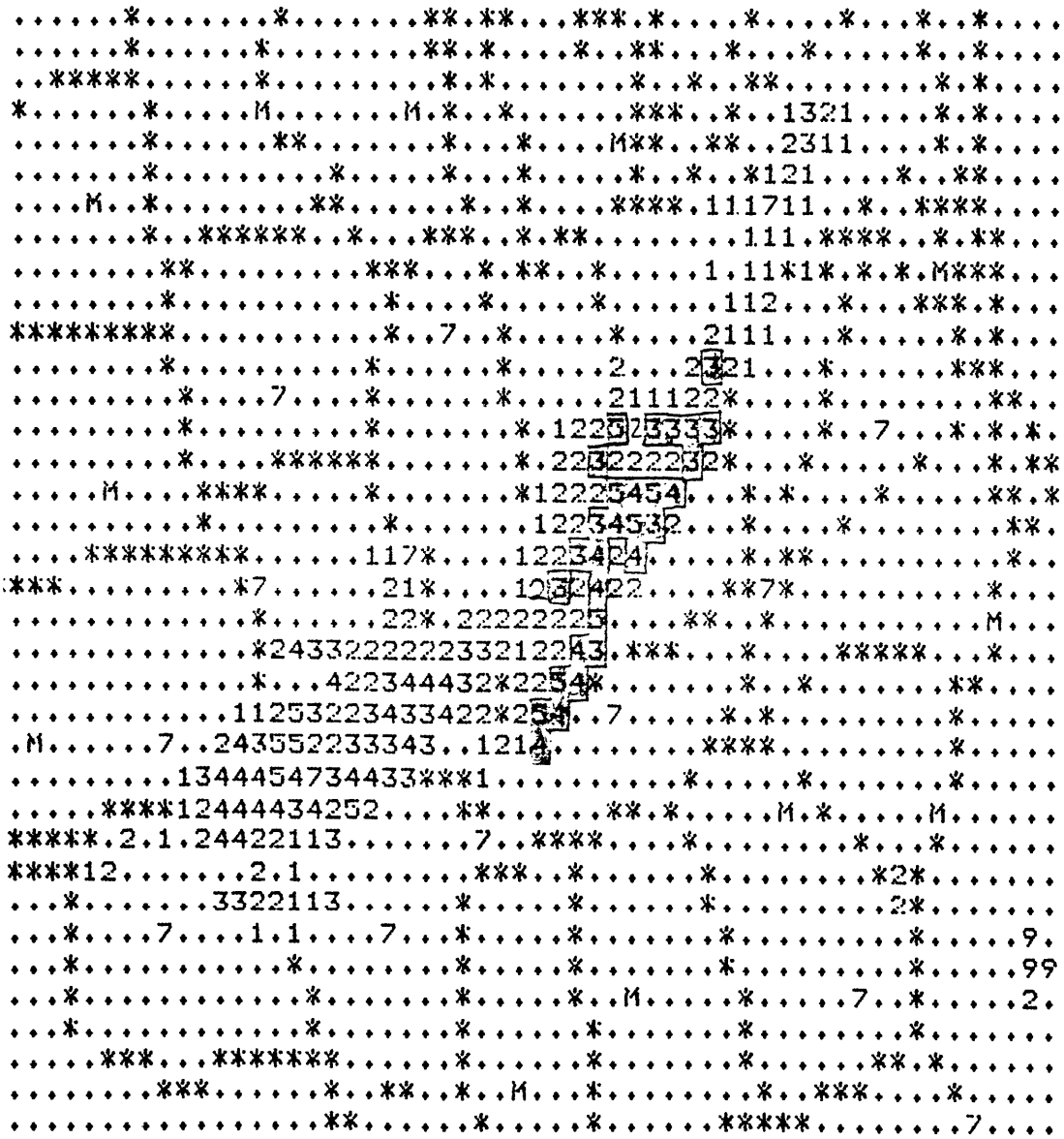

Figure 28. Surface map, 27 August 1982, 0900 GMT. Details similar to fig. 25.

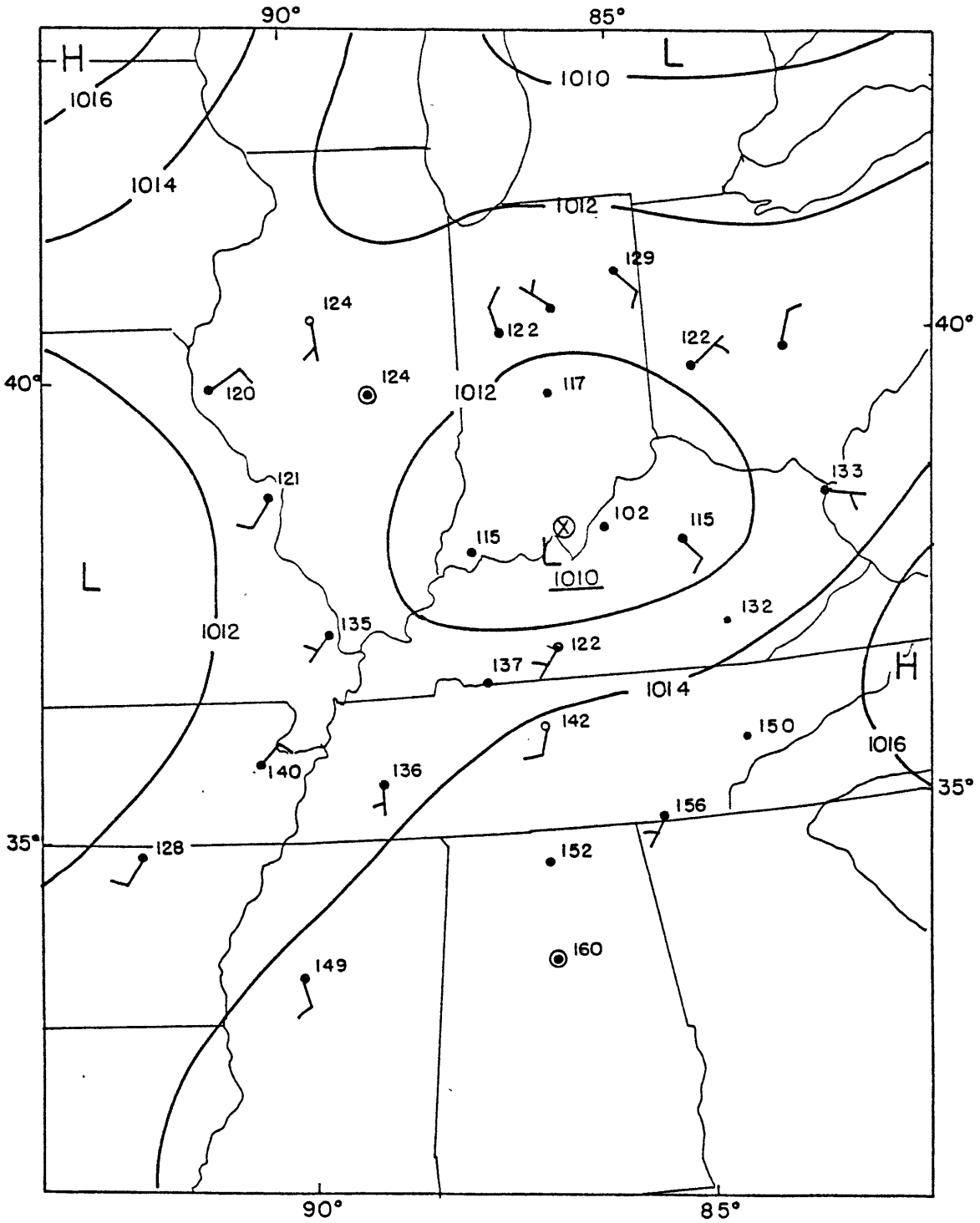
90°
85°
H
1016
1014
L
1010
1012
129
124
122
122
40°
40°
120
124
1012
117
121
133
102
115
115
1010
L
1012
135
132
122
137
H
1014
142
150
1016
140
136
35°
156
35°
128
152
160
149
90°
85°

Figure 29. Infrared satellite picture, 27 August 1982, 1201 GMT. Enhanced areas indicate cloud top temperatures less than -32° C.

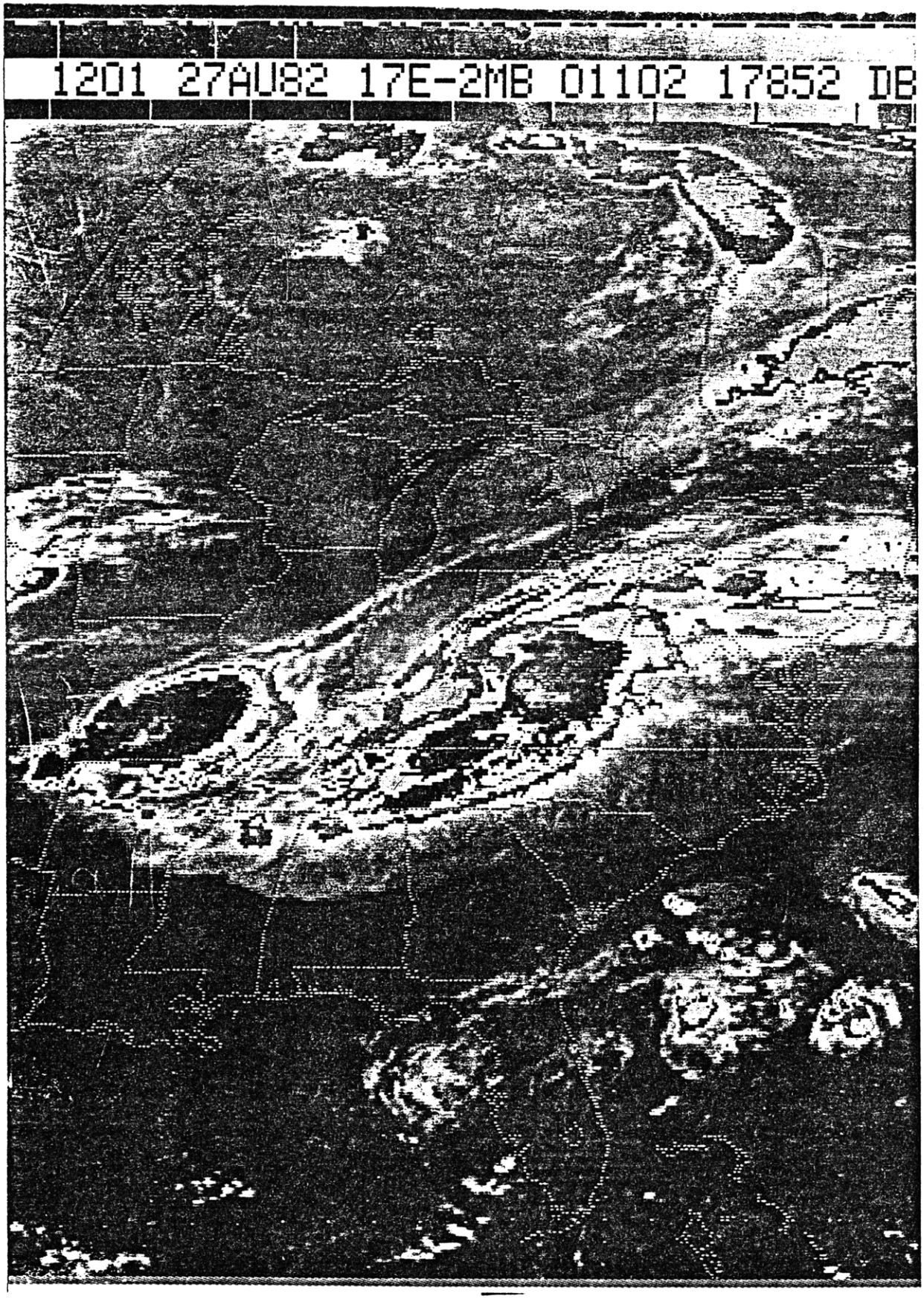
1201 27AU82 17E-2MB 01102 17852 DB

Figure 30. Radar map, 27 August 1982, 1235 GMT. Details similar to fig. 13.

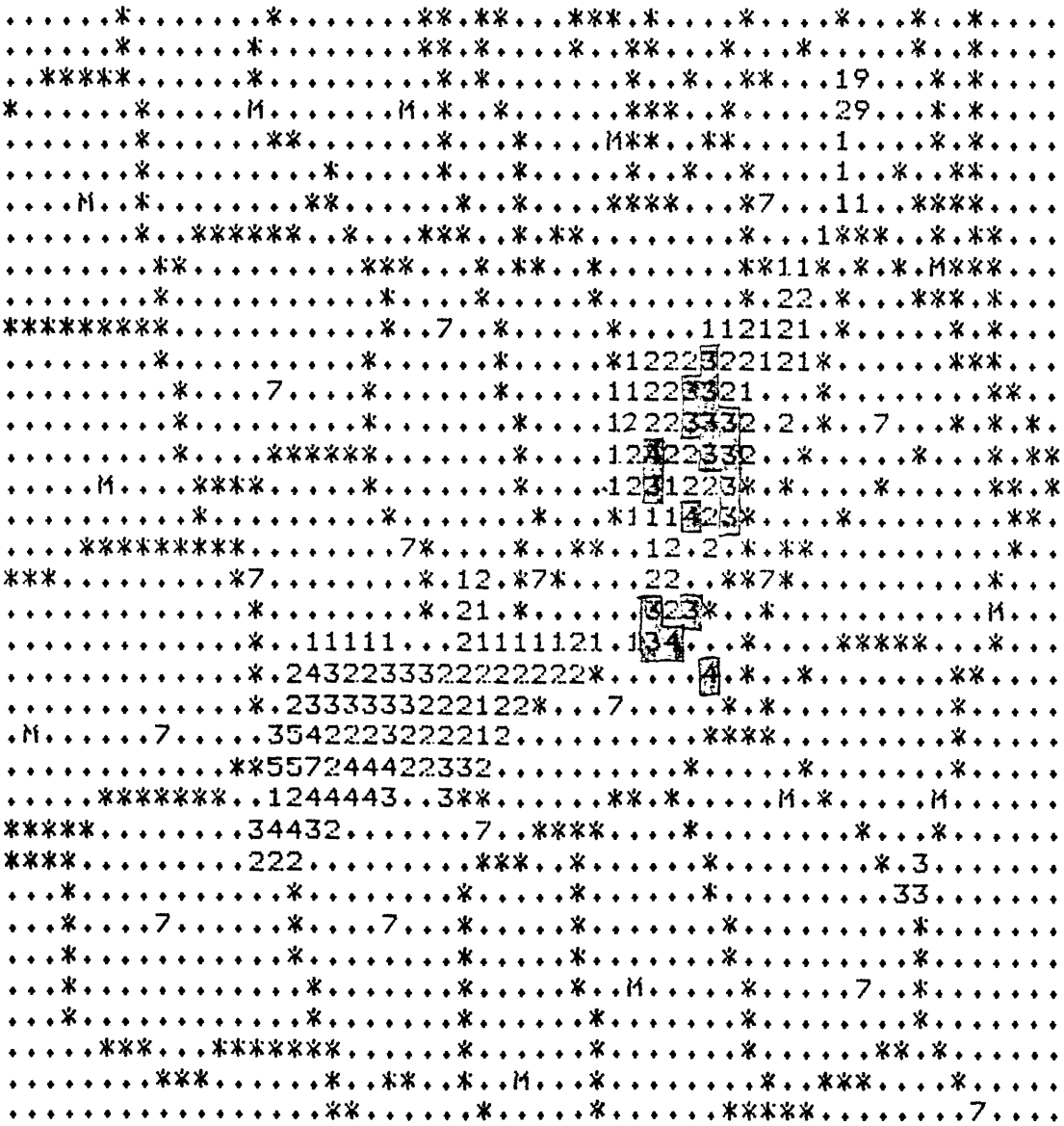

Figure 31. Surface map, 27 August 1982, 1200 GMT. Details similar to fig. 25.

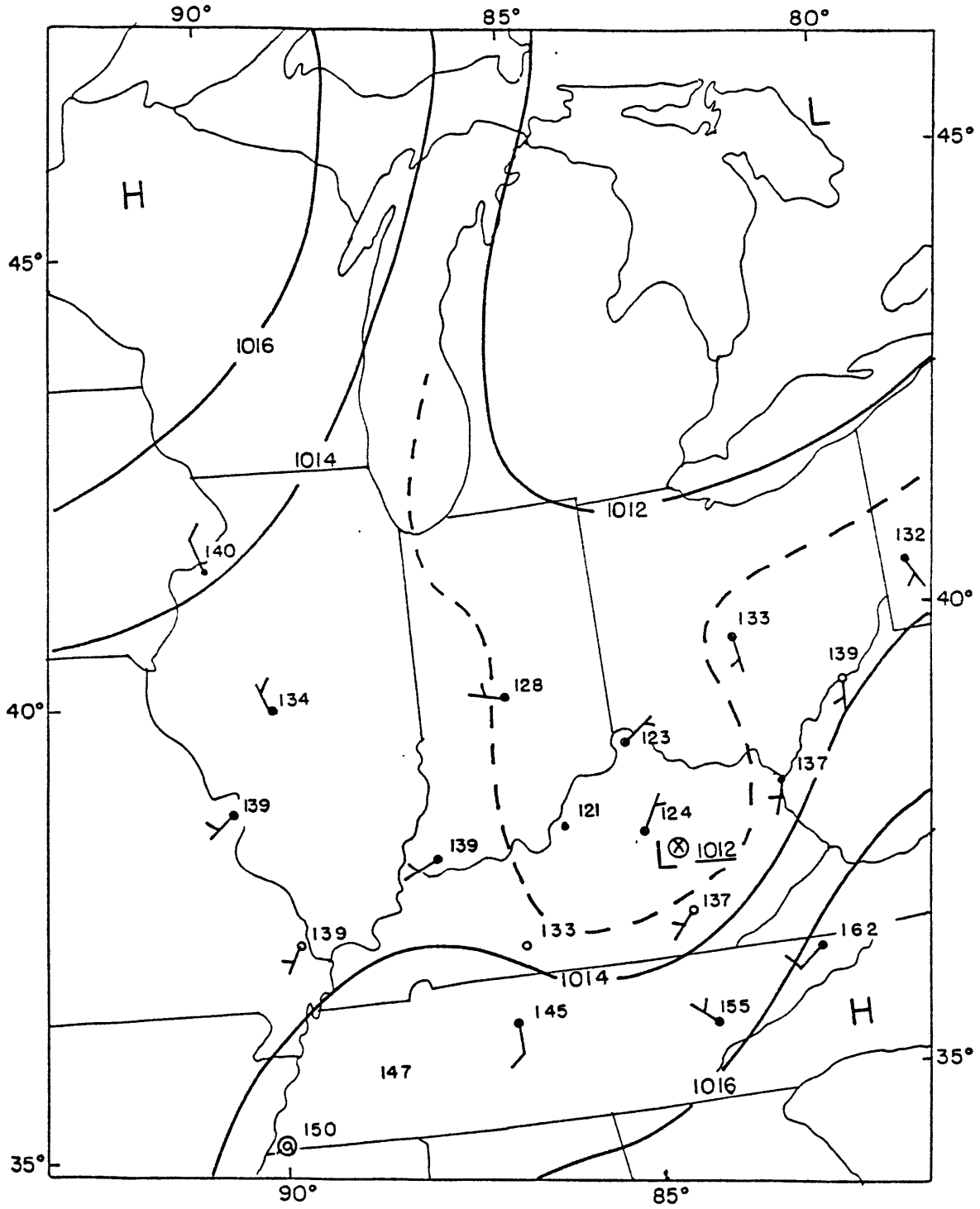
90°
85°
80°
45°
40°
35°
H
L
1016
1014
1012
140
132
133
139
134
128
123
137
139
121
124
1012
139
137
139
133
162
1014
145
155
H
147
1016
150

the lee side of the MCC, and the beginning of its fast movement. It appears that these events are connected; possibly the collapse of air is creating a gravity wave or a perturbation that is transported by the wind.

8. MCC and tropical cloud cluster similarities

Similarities between MCCs and tropical cloud systems have been observed in this study. To make this connection stronger without trying to obscure what appears to be significant differences, Figs. 32 and 33 are presented from Churchill (1982). Data for these figures was derived from the observation of a stationary cloud cluster off the coast of Borneo during the Winter Monsoon Experiment (WMONEX), and favorably agree with the studies of tropical squall lines with large cloud shields. Observations were taken with a single 5.3cm radar, and radar maps of echo intensity were generated at constant altitudes with 16 km^2 resolution. Precipitation was partitioned into convective and stratiform components by an objective technique which compared the reflectivity observed in a grid box with the surrounding data. Generally, a grid box, and a few adjacent boxes, were considered convective if there existed a gradient of reflectivity between a box and nearby boxes which was above a certain threshold. The data for Churchill's study was available to the author of this paper, so a comparison was made between Churchill's results and data taken by the techniques of this study. Qualitatively similar results were obtained, with the differences being a shift of the data to the left by an hour, and a proportionate overestimation of area and rain rates. Both of these changes were caused by the large grid size, which is also more sensitive to broad horizontal trends. The fundamental results, however, and the similarities between these figures and Figs. 5 and 6 are not changed. MCCs and tropical cloud systems do exhibit similar radar time series behavior with the implication that similar processes are occurring.

Figure 32. Area of convective and stratiform rain for WMONEX cloud cluster, 09-10 December 1978 from Churchill (1982).

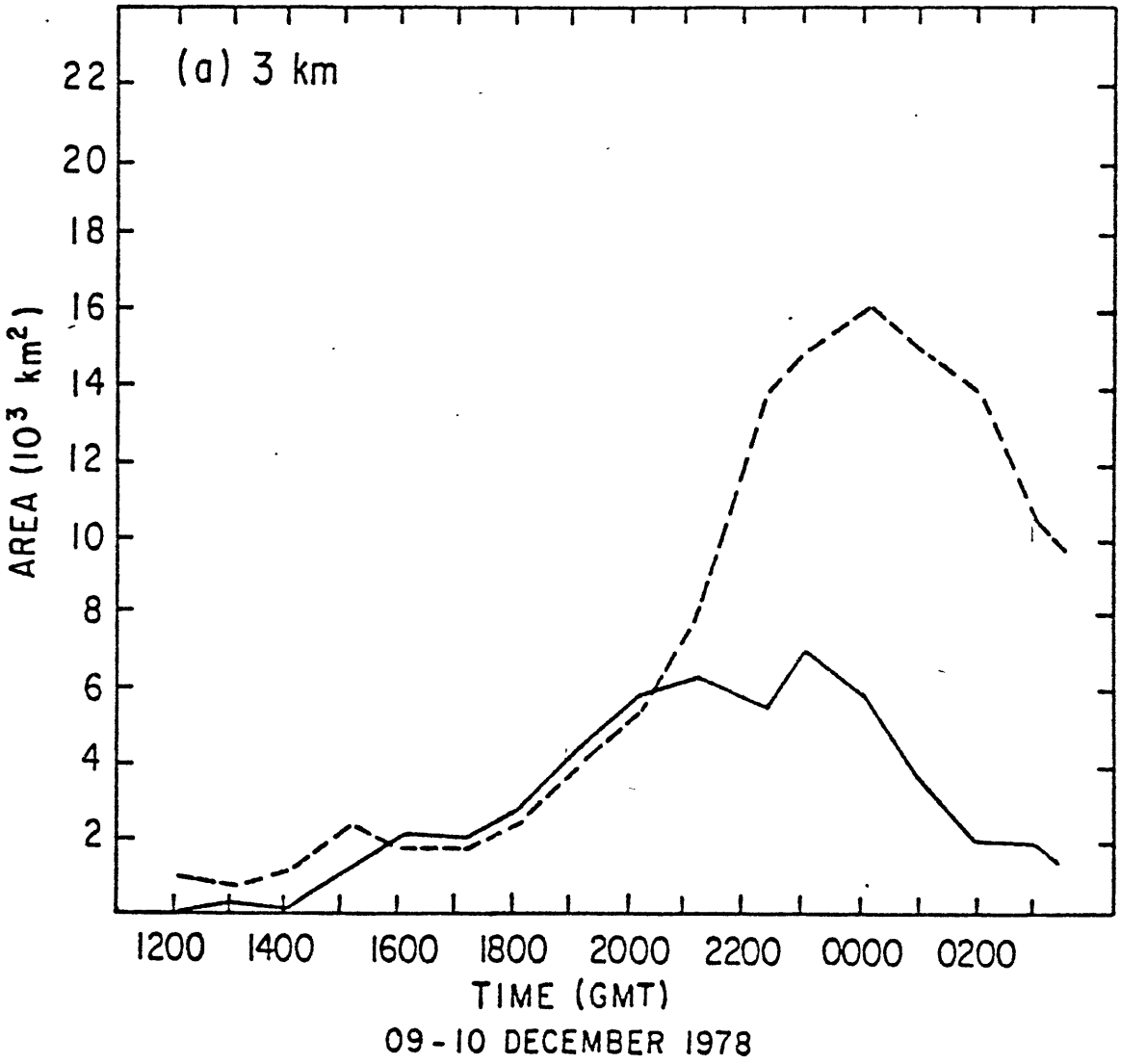

Area covered by stratiform precipitation (dashed curve) and convective precipitation (solid curve) at (a) 3 km, (b) 7 km, (c) 9 km and (d) 11 km above sea level. Objectively determined from the MIT land-based radar data.

Figure 33. Total convective and stratiform rain rates for WMONEX cloud cluster, 09-10 December 1978 from Churchill (1982).

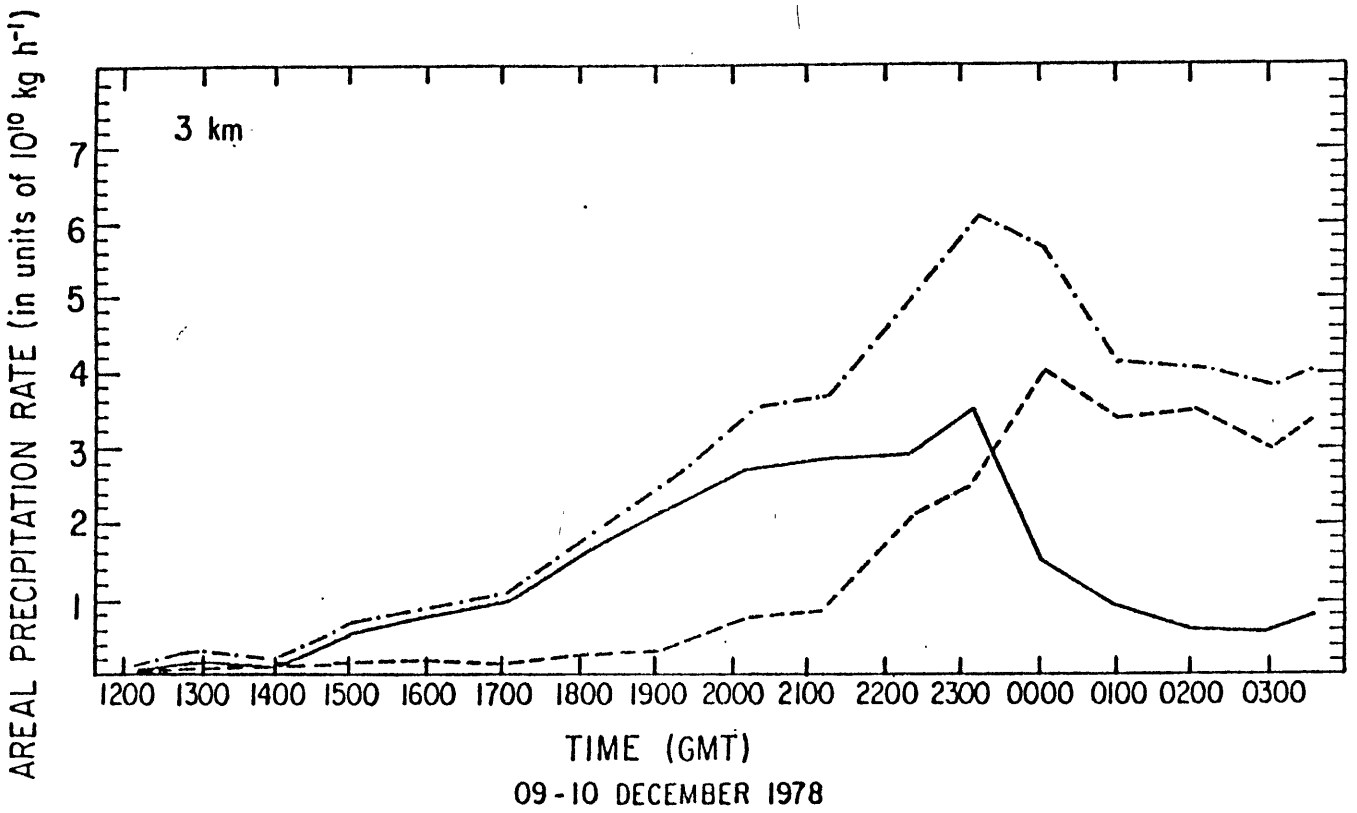

Area-integrated precipitation rate for cloud cluster B at 3 km. The top (dot-dashed) line represents the sum of the convective (solid line) and stratiform (dashed line) components of precipitation.

9. Discussion

Considering the results of the previous sections, it is now possible to derive a more complete model of an MCC. This model does not reflect the behavior of all mesoscale convection that is classified MCC, but it does represent a large subclass of storms whose characteristics are identifiable and repeatedly observed. Individual storms will slightly deviate from the model, and larger deviation within a storm whose basic character fits the model are probably related to atmospheric processes acting independent of the MCC. An example of this is the case of a cold front moving into the late phase stratiform rain, resulting in convection occurring when the model predicts none in this area.

A description of the model MCC follows; the setting is the overall environment described by Maddox (1981):

a. Early Phase

1.) In a favorable environment a small group of very intense cells begins growing. Within a short time an anvil forms, streaming off to the NE, the direction of the mean tropospheric flow. Either simultaneously or slightly later, a secondary convective area forms downwind and to the right of the first. The meso-B scale numerical model of Fritsch and Chappell also suggests the secondary convective area (Fig. 34).

2.) Convection continues to expand. Most of this growth occurs on the windward side of the storm in a loosely defined line which is expanding northward. This growing line is the source of most of the anvil cloud. These characteristics are clearly the same as the model of a tropical squall line proposed by Leary and Houze (1979). See Fig. 35. Additional

Figure 34. Convective rain from Fritsch and Chappell's (1980) mesoscale numerical model.

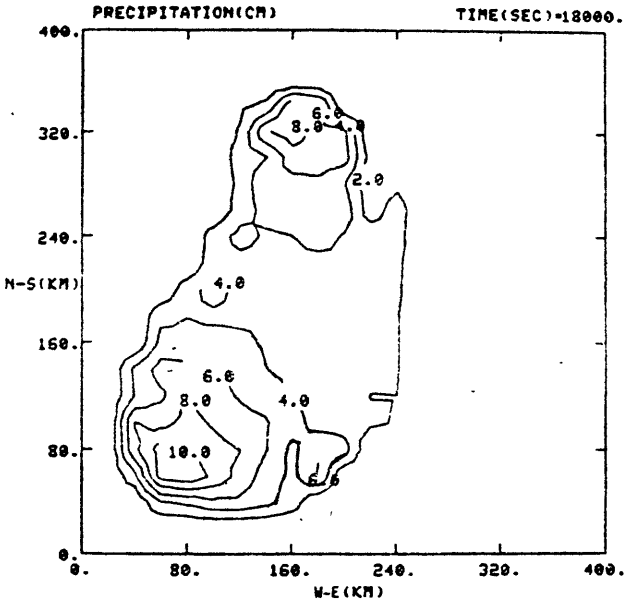

Convective precipitation (cm). Amounts shown are the total for the 2 h period of convection.

Figure 35. Tropical squall line model from Leary and Houze (1979).

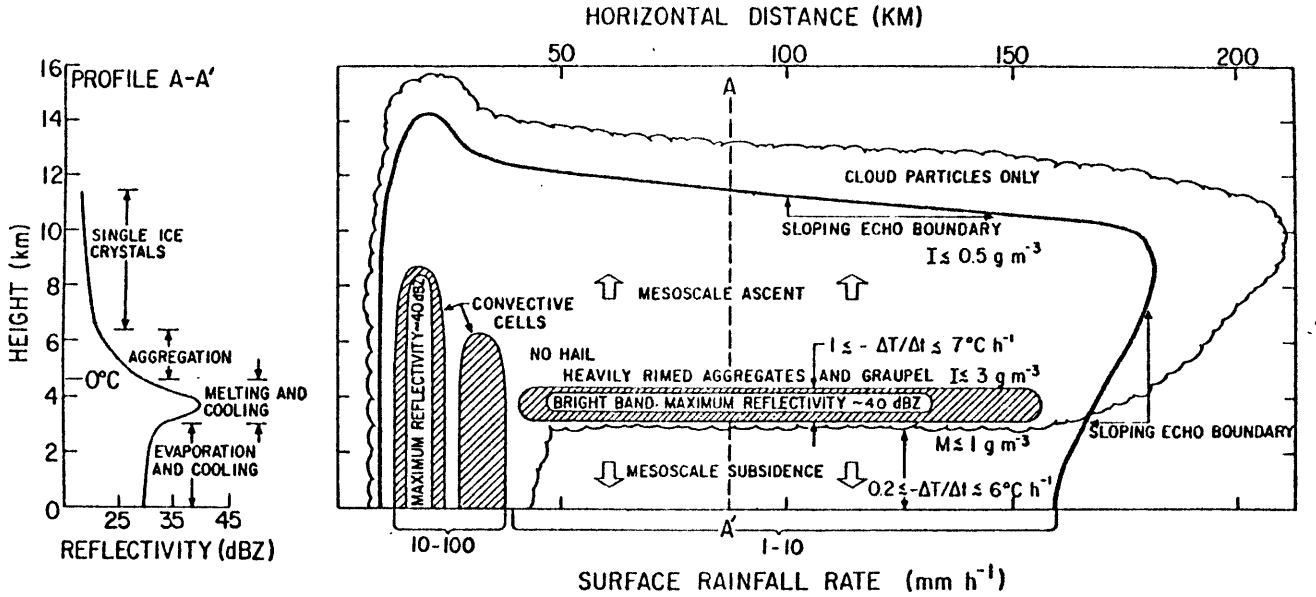

Schematic vertical cross section and vertical profile of radar reflectivity (along dashed line A–A′ in the cross section) in horizontally uniform precipitation associated with an anvil cloud. The anvil cloud occurs to the rear of intense convective cells propagating in the direction from right to left in the figure. The dark solid line is the contour of minimum detectable radar echo, lighter solid lines and shading indicate contours of higher reflectivity, and the scalloped line indicates the cloud boundary.

evidence for the existence of this type of structure in midlatitudes can be found in the model from the observations of Pedgley (1962) (Fig. 36). Range height indicator displays of the large stratiform rain areas in midlatitudes and their similarity to tropical mesoscale structures can be found in Leary (1980) and Lepage and Leary (1981). Fig. 37 is an example from Leary (1980).

The secondary convective area also continues to grow, with lesser convection forming along the SE side of the MCC. Another example of these features can be found in the MCC-like mesoscale system studied by Fujita and Brown (1958). Mesosystem 416 in Fig. 38 shows the structure just discussed -- basically a two-rain area structure, with the secondary rain area to the NE (outside the dashed line, also refer to Fig. 36 and note cumulus clouds forming at the edge of the high stratiform clouds), and lesser convection to the SE, and the implied convection in the trough on the west side of the large rain area. The end of this phase is marked by the peak in the convective rain rate.

b. Transition Phase

1.) A mesolow has formed aloft and is best indicated by the surface low which becomes preferentially located between the large rain area and the secondary convection. The analysis of Fujita and Brown indicates that the surface low moves from the west side of the large rain area to a position between the large area and the secondary convection. See Figs. 38 through 40. It is not clear what the mesolow aloft is doing at this time; probably its formation and movement are regulated by the latent heat release. From the movement of the surface low it seems likely that the low aloft is first strongest near the convection on the west side of

Figure 36. Model of mature mesoscale convective area from Pedgley (1962).

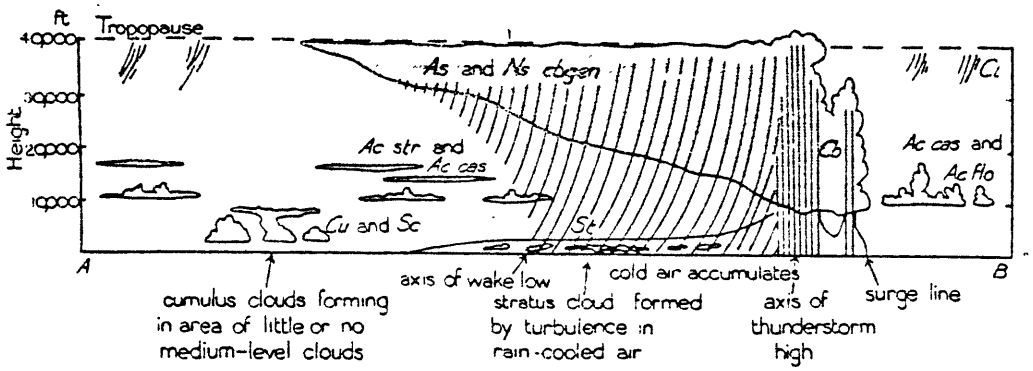

—VERTICAL CROSS-SECTION

Figure 37. Range height indicator view of a midlatitude mesoscale anvil cloud by Leary (1980).

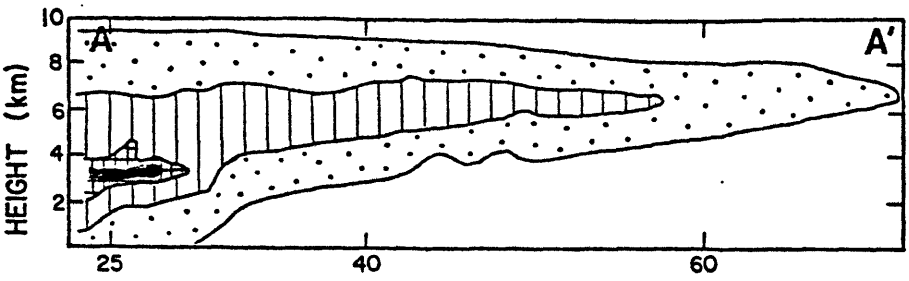

(a) DISTANCE FROM SNYDER RADAR (km)

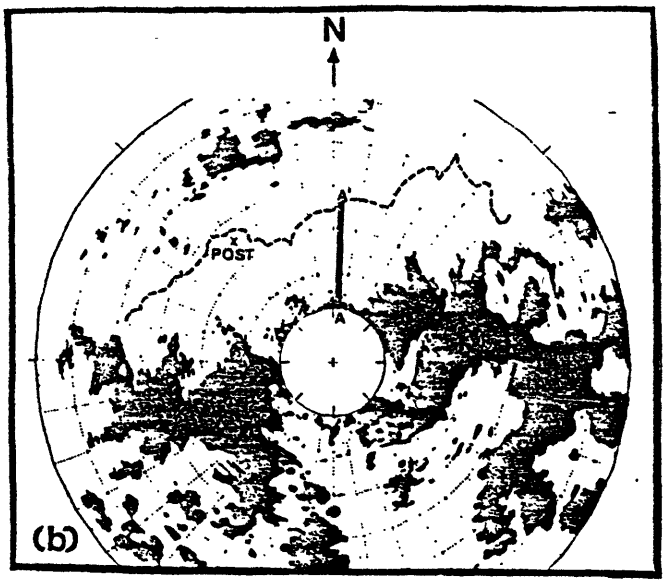

RHI (a) and low-level (1°) PPI (b) displays derived from Snyder digital radar data for 2104 GMT, 8 July 1977. RHI lies along line A-A' shown in PPI. Outside countour on RHI is boundary of weakest detectable echo, and inside contours are for 25, 30, and 35 dBZ. Echo boundary on PPI is 25 dBZ. Range marks on PPI are at 25, 40, 60, 80, 100, 120, and 130 km. The heavy dashed line on PPI outlines the maximum horizontal extent of precipitation particles detectable by radar in the anvil cloud aloft.

Figure 38. Surface and precipitation analysis of mesoscale convection by Fujita and Brown (1958), 5 June 1953, 0400 GMT.

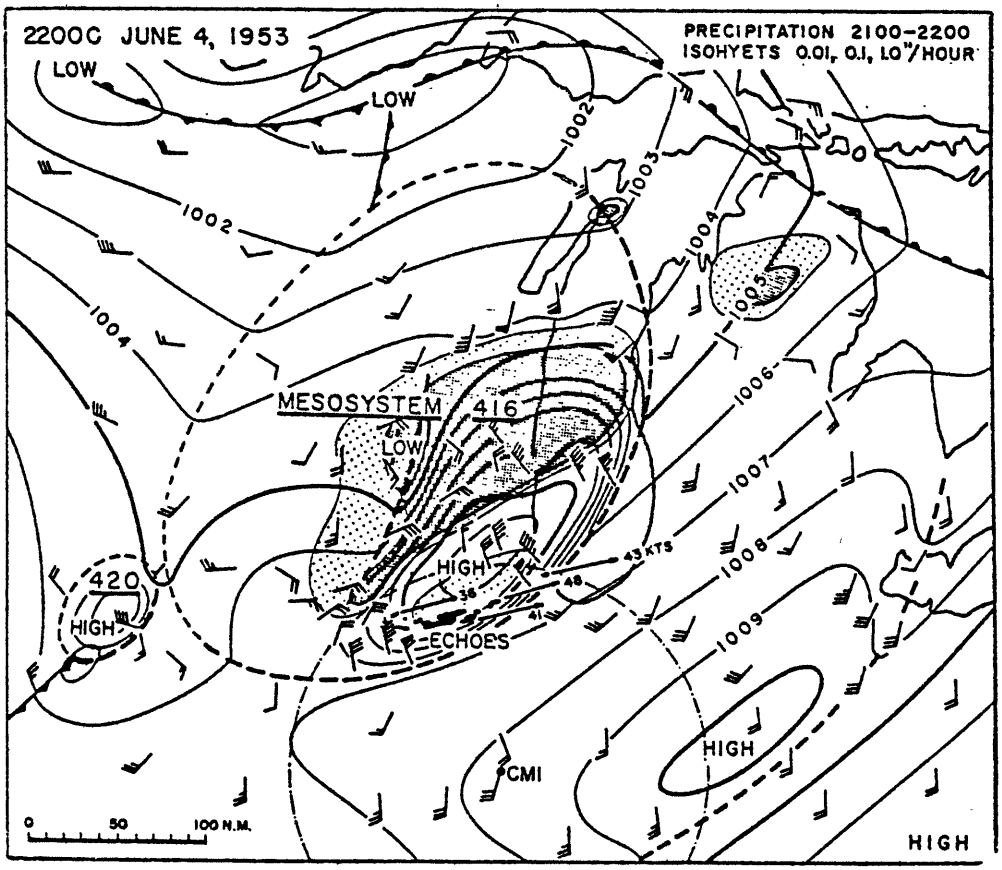

Surface chart for 2200 CST 4 June 1953.

Figure 39. Surface and precipitation analysis of mesoscale convection by Fujita and Brown (1958), 5 June 1953, 0700 GMT.

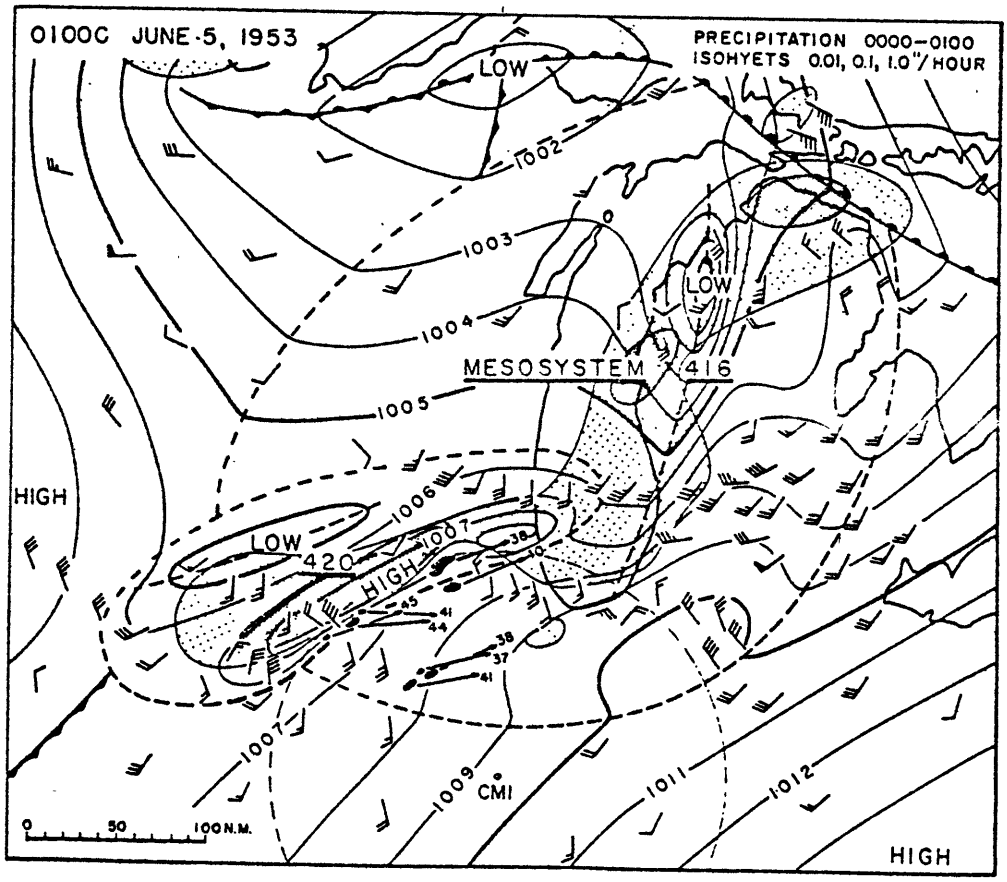

Surface chart for 0100 CST 5 June 1953.

Figure 40. Movement of meso-pressure areas in mesosystem 416 from Fujita and Brown (1958).

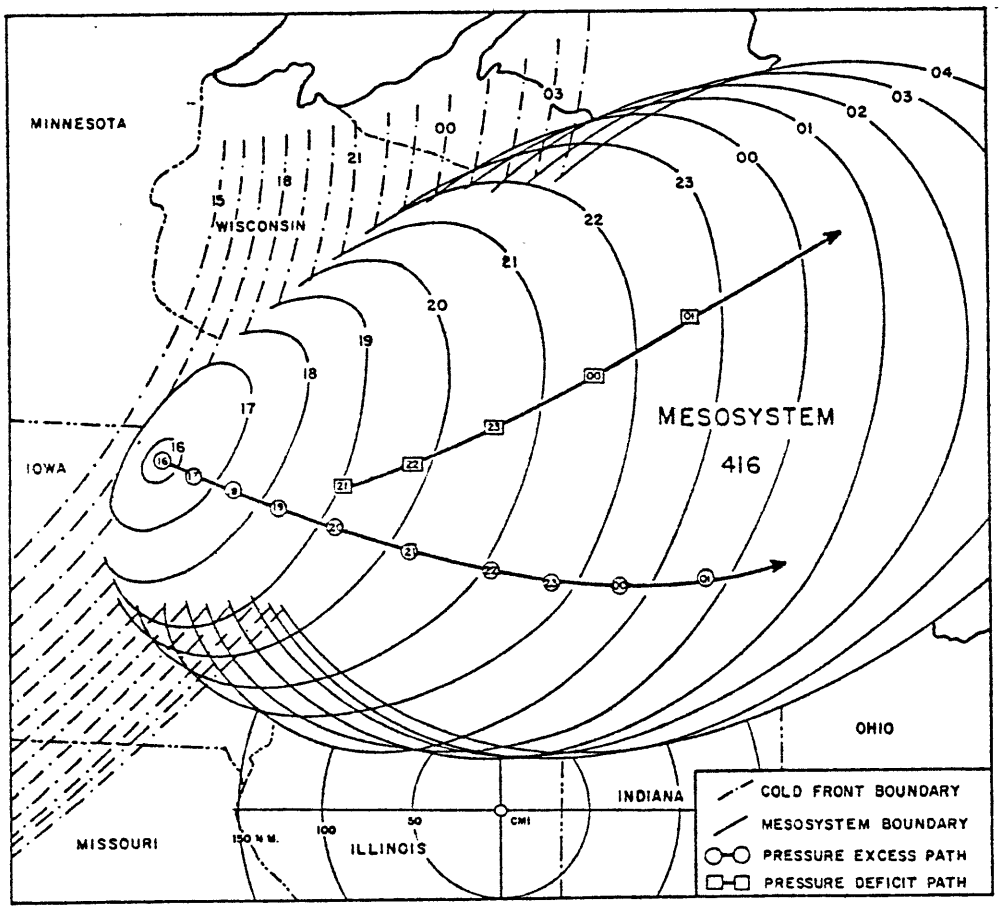

Isochrones of cold front and Mesosystem 416 and paths of excess and deficit pressure.

the storm then moves east as the center of maximum latent heat release moves east because of the increase in stratiform rain. Transport by the wind may also play a part in moving the low aloft.

At the beginning of transition, the low and its circulation are significant enough to begin altering the environment which is supporting the convection. The convection on the west side of the MCC begins to decay, and a convective line forms on the SE side. Both of these occurrences can be explained by the circulation around the low, i.e., more stable air is drawn in from the north, killing the west convection, and the cold air under the stratiform rain is pushed into warm air to the southeast. Thus, a strong discontinuity along which convection forms is created. During this time the total rain and cloud area have reached their maximum extent. The end of this period occurs when the stratiform rain area stops growing. Although the stratiform rain can continue growing after the convection begins to decrease, the upwind source of convection supplied moisture seems to influence the time span in which the stratiform rain will grow. When the west side convection begins to decay, the overall growth of the rest of the storm soon stops. The largest and longest lasting storms are those where the west side convection is regenerated, usually, by a feature independent of the MCC.

c. Late Phase

Decaying stratiform rain areas and squall line characteristics of the remaining convection are the most distinguishing feature of the MCC at this time. Widespread stratiform rain can not be supported when the convection is oriented parallel with the mean flow of the MCC environment. The line propagation is roughly perpendicular to its axis and may persist

for many hours, occasionally producing severe weather (the maximum number of severe events, however, occur in the earlier phases of the storm). As seen in the previous section, a large cloud mass may form at the northern edge of the line and slightly ahead of the surface mesolow, but this phenomenon, and other characteristics of the MCC, appear with varying intensities related only in a general way to overall storm size.

10. Summary and conclusions

A large subclass of storms which have been identified as MCCs by the criteria of Maddox do have identifiable and repeatedly observed convective and stratiform precipitation cycles and structures. The early phase of these storms appear identical to tropical squall lines, or cloud clusters with convection mainly on one side. While, in the late phase, the active region of the precipitation takes on the character of a weak midlatitude squall line. Mesoscale circulations, dominated by a mesolow in the lower troposphere, appear mostly responsible for the transformation of the MCC from a tropical equivalent storm to a storm resembling a midlatitude squall line.

The usefulness of Maddox'(1980) MCC criteria, other than its success at identifying the largest mesoscale convective systems when the criteria is selectively applied to cloud area in the central United States, must be questioned. First, the area of cloud top with temperature -32° C or less always overestimates the total rain area, with the greatest overestimation occuring in storms where the late phase convective line is in the center of the MCC. In these and similar cases the large area of cloud SE of the line has little, if any, stratiform or convective rain. Second, at Maddox' initiation and termination times, large horizontal areas are already, or are still, being affected by these storms. Initiation does not correspond to the start of an identifiable process or change in character of the storm, and occasionally occurs after the convection has begun to decrease. Similar statements can be made about termination with, again, the observation that at termination a significant meteorological phenomenon is still occurring and may continue for some length of time. Furthermore,

this misleading labeling of start and stop time obscures the facts that these systems generally grow in a preexisting circulation, a circulation is left after Maddox' cloud characteristics are gone, and the remaining circulation can be the basis for later concentration of convection (Bosart and Sanders, 1981). Third, there is no reason to believe that mesoscale convective systems which meet Maddox' MCC criteria are fundamentally different in structure and processes from other systems which do not. Detailed examination of non-MCC cases was not done in this study, but the apparent applicability of many results from mesoscale studies of all scales suggests that less emphasis should be placed on studying mesoscale convection by size and more emphasis put on understanding fundamental convective structures and processes.

APPENDIX

Many other MCC features were observed in this work, but there was not sufficient time or data to thoroughly document them. A short list of these observations is written below with the hope that other investigators might find them useful.

a. The first strong convective areas tended to occur in, or on the border of, a preexisting low level cloudy area which was usually trackable for many hours before the first storms.

b. Small linear cloud lines were sometimes observed to move into the west side of an MCC and trigger new convection, thus enlarging the MCC and making it last longer. The best example of this was the case of 6/7 May 78.

c. It has been stated that the low level jet is somehow tied into the maximum convection of an MCC, but this connection becomes questionable when it is noticed that the peak in convection in the average storm occurs before the climatological peak of the low level jet.

d. In the cases where much of the MCC was aloft above a cold front, the late phase convective line would only be well organized to the south of the surface cold front. This suggests surface friction is responsible for keeping the line well organized.

e. The likeness between the early phase of the MCC and tropical squall lines has now been well documented, but it is not clear if the distinguishing feature of the MCC, the mesolow aloft, also develops in some tropical cases. It is suspected that lows do sometimes form from tropical mesosystems, perhaps the stronger of these cases become tropical storms.

ACKNOWLEDGMENTS

I sincerely want to thank Dr. Sanders for introducing me to the topic of mesoscale convection in his synoptic meteorology class, and supporting my unorthodox study of the subject. Dr. A. Thompson of Texas A&M University and Mr. Walsh from the National Climatic Center were instrumental in supplying data for this study and helped me many times with "final" requests. Isabelle Kole's drafting of my figures was greatly appreciated. Thanks, also, to the taxpayers of the United States who paid my salary and tuition through the offices of the U.S. Air Force, but I would never have completed any of this without the love and sacrifice of my wife, Joae, and my family.

REFERENCES

Bosart, L.F. and F. Sanders, 1981: The Johnstown flood of July 1977: A long-lived convective storm. J. Atmos. Sci., 38, 1616-1642.

Churchill, D.D., 1982: Development and structure of winter monsoon cloud clusters. University of Washington Master of Science Thesis. 200pp.

Fritsch, J.M., and C.F. Chappell, 1980: Numerical prediction of convectively driven mesoscale pressure systems, Part II: Mesoscale model. J. of Atmos. Sci.,37, 1734-1762.

Fujita, T., and H.A. Brown, 1958: A study of mesosystems and their radar echoes. Bull. Amer. Meteor. Soc.,39,538-554.

Houze, R.A., Jr., 1977: Structure and dynamics of a tropical squall line system. Mon. Wea. Re.,105,1541-1567.

Kreitzberg, C.W. and D.J. Perkey, 1977: Release of potential instability: Part II. The mechanism of convective/mesoscale interaction. J. Atmos. Sci.,34, 1569-1595.

Leary, C.A., 1980: Structural Similarities between mesoscale convective systems observed over the Texas south plains during HIPLEX and over the tropical ocean during Gate. Preprints Nineteenth Conf. on Radar Meteorology,AMS,384-389.

Leary, C.A., and R.A. Houze, 1979: Melting and evaporation of hydrometeors in precipitation from the anvil clouds of deep tropical convection. J. Atmos. Sci., 36, 669-679.

Lepage, M.F., and C.A. Leary, 1981: Evolution of a midlatitude mesoscale convective system. Preprints Twenthieth Conf. on Radar Meteorology, AMS, 243-250.

Maddox, R.A., 1980: Mesoscale convective complexes. Bulletin of the American Meteorological Society,61, 1374-1387.

Maddox, R.A., 1981: Structure and life-cycle of midlatitude mesoscale convective complexes. Colorado State University Atmospheric Science Paper No.336.311.

Pedgley, D.E., 1962: A meso-synoptic analysis of the thunderstorms on 28 August 1958. Geophysical Memoir No. 106, Meteorological Office 711, 74pp.

U.S. Dept. of Commerce, 1978: National Weather Service Radar Code User's Guide, 24pp.